

Trainability and Expressivity of Hamming-Weight Preserving Quantum Circuits for Machine Learning

Léo Monbroussou,^{1,2} Jonas Landman,^{3,4} Alex B. Grilo,¹ Romain Kukla,² and Elham Kashefi^{1,3}

¹Laboratoire d'Informatique de Paris 6, CNRS, Sorbonne Université, 4 Place Jussieu, 75005 Paris, France

²CEMIS, Direction Technique, Naval Group, 83190 Ollioules, France

³School of Informatics, University of Edinburgh, 10 Crichton Street, Edinburgh, United Kingdom

⁴QC Ware, Palo Alto, USA and Paris, France

(Dated: September 28, 2023)

Quantum machine learning has become a promising area for real world applications of quantum computers, but near-term methods and their scalability are still important research topics. In this context, we analyze the trainability and controllability of specific Hamming weight preserving quantum circuits. These circuits use gates that preserve subspaces of the Hilbert space, spanned by basis states with fixed Hamming weight k . They are good candidates for mimicking neural networks, by both loading classical data and performing trainable layers. In this work, we first design and prove the feasibility of new heuristic data loaders, performing quantum amplitude encoding of $\binom{n}{k}$ -dimensional vectors by training a n -qubit quantum circuit. Then, we analyze more generally the trainability of Hamming weight preserving circuits, and show that the variance of their gradients is bounded according to the size of the preserved subspace. This proves the conditions of existence of Barren Plateaus for these circuits, and highlights a setting where a recent conjecture on the link between controllability and trainability of variational quantum circuits does not apply.

I. INTRODUCTION

Variational quantum circuits (VQCs) are promising candidates for near term quantum computing [1], but existing and near-term quantum devices still offer limited resources to implement important tasks for quantum machine learning (QML), such as encoding and training. Considering fault-tolerant quantum computation, more advanced QML algorithms that present potential to achieve a quantum advantage exist. The key step of some of these “quantum linear algebra” algorithms [2–4] is amplitude encoding, where the input vector’s components become the quantum amplitudes of the input state in the computational basis. Amplitude encoding on the entire Hilbert space is unlikely to be achieved in the near term, and recent work proposed to use amplitude encoding in small subspaces [5–7]. In other methods for variational QML, the data encoding is done by putting directly the vector component as the gate parameters, which leads to some limitations [8, 9].

In this work, we propose a method to achieve the amplitude encoding of any $\binom{n}{k}$ -dimensional vector using n qubits by training a VQC made of Hamming weight (HW) preserving gates. In recent work [5], a n -qubit quantum data loader using HW preserving gates was presented to encode any n -dimensional vector using a VQC, but without training. HW preserving quantum circuits allow one to restrict the state created to a superposition of states of the same HW as the input, i.e., to maintain the number of qubits in state $|1\rangle$ at the same time. Such subspace invariant quantum circuits can tackle an important scaling problem with QML methods called Barren Plateaus (BP) [10]. It has been recently shown that one can avoid BP while using input data on an invariant subspace of low dimension under certain conditions on their controllability and expressivity [11]. However, knowing

if HW preserving VQCs are prone to BP without those assumptions is still an open question that we tackle in this work.

One of our main results can be informally stated as follows: for a n -qubit circuit made of specific HW preserving gates (RBS and FBS), in the subspace spanned by Hamming weight k , the gradient of the cost function vanishes as $O(1/\binom{n}{k})$. This is neither exponentially decreasing with n (Barren Plateau), nor quadratically decreasing as one could have expected for the FBS case, despite its lower controllability.

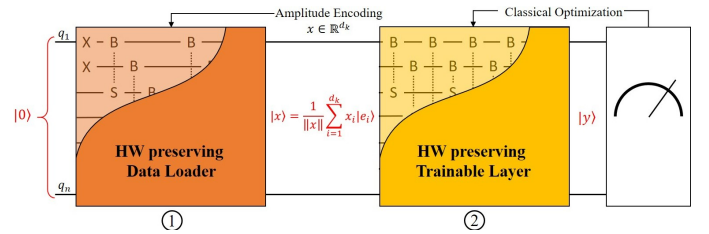


FIG. 1: Representation of a Hamming weight preserving quantum circuit for Quantum Machine Learning purposes: (1) is the encoding part trained to represent the classical input, and (2) is the trainable layer or quantum neural network. The gates represented with B and S signs are RBS.

We first develop in Section II a framework to design a quantum data loader on any invariant subspace of dimension $\binom{n}{k}$, with a n -qubit circuit and k the chosen HW (see Fig. 1). In addition, we propose a study of the trainability for HW preserving VQCs in Section III (this concerns both blocks in Fig. 1). We show that one could avoid BP using HW preserving gates according to the choice of the subspace used for the encoding without any hypothesis on the controllability or expressivity of the VQC.

Related work

The preservation of the HW is a symmetry that we use in this work in order to propose encoding and trainable layers with theoretical guarantees on their trainability. Quantum machine learning models that present symmetries have been proposed as potential more efficiently trainable than common models [12–16]. More recently, problem-inspired ansatz have been studied using tools from quantum optimal control to highlight a link between the dimension of their corresponding dynamical Lie algebra and their trainability [11] using a certain set of hypothesis. One main conjecture left open in [11] concerned the link between trainability and controllability *in a subspace*. Very recent works just prove that this conjecture applies to many commonly used ansatzes [17, 18] such as the Hamiltonian Variational Ansatz [19], Quantum Alternating Operator Ansatz [20, 21], and many equivariant quantum neural networks. However, in our work, we show that this conjecture is not respected in the case of HW preserving ansatzes, which received increasing attention [5–7, 22]. Our results are consistent and independent of the two works recently released [17, 18] as HW preserving ansatzes don't respect the assumptions these papers are relying on. One can notice that [18] studies the same ansatzes as we do (see their Appendix C), and propose an upper-bound on their controllability in a specific setting. In Section III, we give tighter theoretical guarantees on the trainability of those ansatzes, using a different analytical proof. See Section V for discussion.

II. SPACE-EFFICIENT AMPLITUDE ENCODING.

We first define the Amplitude Encoding and HW preserving quantum data loaders. Then we show how to achieve it efficiently using HW preserving gates and their subspace preserving properties.

A. Hamming weight preserving quantum data loaders

Let us first define the Amplitude Encoding scheme and explain what are HW preserving quantum data loaders.

Definition 1 (Amplitude Encoding). *A data loader is a parameterized n -qubit quantum circuit that, given a classical vector $x = (x_1, \dots, x_d) \in \mathbb{R}^d$, prepares the quantum state:*

$$|x\rangle = \frac{1}{\|x\|} \sum_{i=1}^d x_i |e_i\rangle, \quad (1)$$

where $|e_i\rangle$ are n -qubit orthogonal quantum states.

Definition 2 (Data Loader in a HW preserving subspace). *We define a n -qubit data loader in the subspace*

of HW k , the quantum circuit that performs amplitude encoding on the basis:

$$B_k^n = \{|e\rangle | e \in \{0, 1\}^n \text{ and } HW(e) = k\} \quad (2)$$

with $d_k = |B_k^n| = \binom{n}{k}$.

For example, when considering $n = 3$ qubits and a HW $k = 2$, the resulting basis state is:

$$B_2^3 = \{|110\rangle, |101\rangle, |011\rangle\}$$

One could use the Reconfigurable Beam Splitter (RBS) gate to perform such an encoding. This HW preserving gate is easy to implement or native on many quantum devices. Notice that our results hold for another HW preserving gate named the Fermionic Beam Splitter (FBS) which was already used for QML application in [22] but has less good properties in term of controllability (see Section II B and Appendix C).

Definition 3 (Reconfigurable Beam Splitter gate). *The Reconfigurable Beam Splitter (RBS) gate is a 2-qubit gate that corresponds to a θ -planar rotation between the states $|01\rangle$ and $|10\rangle$:*

$$RBS(\theta) = e^{i\theta H_{RBS}} = \begin{pmatrix} 1 & 0 & 0 & 0 \\ 0 & \cos(\theta) & \sin(\theta) & 0 \\ 0 & -\sin(\theta) & \cos(\theta) & 0 \\ 0 & 0 & 0 & 1 \end{pmatrix} \quad (3)$$

with its corresponding Hamiltonian:

$$H_{RBS} = \begin{pmatrix} 0 & 0 & 0 & 0 \\ 0 & 0 & -i & 0 \\ 0 & i & 0 & 0 \\ 0 & 0 & 0 & 0 \end{pmatrix} \quad (4)$$

Definition 4 (Fermionic Beam Splitter). *Let $i, j \in [n]$ be qubits and $S = s_1 \dots s_n \in \{0, 1\}^n$ a binary word corresponding to a single state $|S\rangle$ with n the total number of qubits. Then the Fermionic Beam Splitter (FBS) acts on the qubits i and j as the following unitary:*

$$FBS_{i,j}(\theta) |S\rangle = \begin{pmatrix} 1 & 0 & 0 & 0 \\ 0 & \cos(\theta) & (-1)^f \sin(\theta) & 0 \\ 0 & (-1)^{f+1} \sin(\theta) & \cos(\theta) & 0 \\ 0 & 0 & 0 & 1 \end{pmatrix} \quad (5)$$

with $f = f_{i,j,S} = \sum_{i < l < j} s_l$

The Hilbert space spanned by a subspace preserving VQC can be expressed as a direct sum of invariant subspaces. By rearranging the order of the computational basis, we can express the HW preserving VQC unitary as a block matrix. Each block is an orthogonal matrix W^k that corresponds to a unitary in the subspace of states of a certain Hamming weight k .

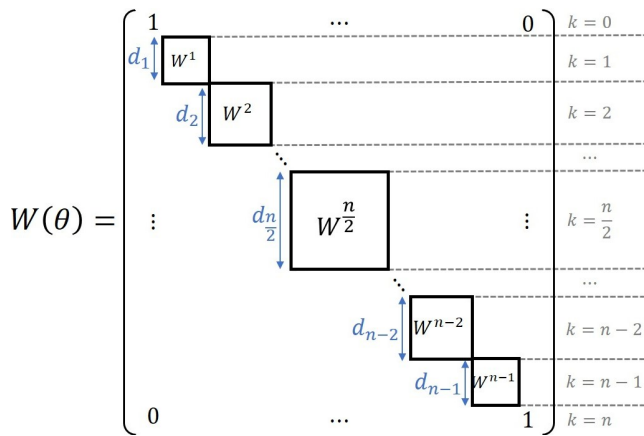


FIG. 2: Block representation of the HW preserving unitaries. \tilde{W} is the $2^n \times 2^n$ unitary corresponding to a n -qubit HW preserving quantum circuit. Each block k is the unitary matrix corresponding to the preserved subspace of HW k , and the state basis B_k^n . Their size are $d_k \times d_k$ where $d_k = \binom{n}{k}$.

We now explain our data loading scheme. First, we initialize the quantum state to be $|e_s\rangle$, a single state of HW k . Then we split off this state onto the states in B_k^n using RBS. In [5], the authors used a similar method on the unary basis B_1^n . Notice that achieving an amplitude encoding with such a basis would allow us to encode many more parameters, namely $\binom{n}{k} \gg n$, in an n qubit state. To design our quantum data loader, we need to ensure that any $\binom{n}{k}$ -dimensional real vector x can be encoded, i.e., that there exists a set of RBS gate parameters $\Theta = \{\theta_1, \dots, \theta_D\}$ such that:

$$W^k(\Theta) |e_s\rangle - \frac{1}{\|x\|} \sum_{i=1}^{\binom{n}{k}} x_i |e_i\rangle = 0, \quad (6)$$

Finding the corresponding set of variational parameters or proving their existence is very hard when $k > 1$, and we discuss how one can try to do it efficiently in future work (see Appendix A). In this work, we focus on the existence of a solution, and we find the solution by defining an equivalent optimization problem that can be solved using a gradient descent based method. Theoretical guarantees to solve the optimization problem easily are described in Section III.

$$\Theta^* = \arg \min_{\Theta} \left\| \frac{1}{\|x\|} \sum_{i=1}^{\binom{n}{k}} x_i |e_i\rangle - W^k(\Theta) |e_s\rangle \right\|_2^2 \quad (7)$$

Notice that the previous cost function does not induce a Barren Plateaus while considering a global cost function [23], as the Hilbert space described by the state of HW k is not exponentially large for small choice of k . We confirm in Section III that a large choice of k results in the existence of Barren Plateaus.

Subspace preserving quantum circuits are easier to simulate in small subspaces than random quantum circuits over the entire Hilbert space [24]. In the case of a HW preserving VQC, the speedup of using a quantum computer grows with k . Classical simulability can be appreciated for the encoding part when combined with a trainable layer that is hard to simulate.

B. Existence of Quantum Data Loader

Previously, we proposed the use of HW preserving ansatz such as a n -qubit RBS based VQC to create a quantum data loader. This circuit will be trained to perform the amplitude encoding of a $\binom{n}{k}$ -dimensional vector with k the chosen HW. In this Section, we give tools to study the existence of a circuit that always presents a solution for our optimization problem given by Eq. (7). More precisely, we show how to know if, given a qubit connectivity and RBS gates, one can design a quantum data loader. If so, we give a method to design the circuit in Section II C.

We propose to use quantum optimal control tools to show that, according to the circuit connectivity, we can prove the existence of a quantum data loader. This method can be generalized to find quantum data loaders for any subspace invariant ansatz. We first define an essential tool to study the controllability of a quantum circuit in the unitary space.

Definition 5 (Dynamical Lie Algebra). *Let us consider that we have an Hamiltonian of the form:*

$$H = H_0 + \sum_{k \geq 1}^G u_k(t) H_k \quad (8)$$

where each u_k is a real function that we can freely choose. We call $\{H_k\}_{k \in [0, G]}$ the set of generators of our quantum system. The Dynamical Lie algebra is defined as:

$$\mathcal{L} = \text{span} \langle iH_0, \dots, iH_G \rangle_{\mathcal{L}} \subseteq \mathfrak{su}(d) \quad (9)$$

with $\langle S \rangle_{\mathcal{L}}$ the Lie closure, i.e., the set of all Lie commutators between the elements in S .

In the case of RBS based quantum circuits, the generators are given by the qubit connectivity as we restrict ourselves to the use of a unique 2-qubit gate (see Fig. 4). We show in Appendix B how to compute the dimension of the DLA. We can restrict this study of the DLA to a particular subspace of HW k . Then, its dimension indicates the maximal number of coefficients we can independently fix in W^k . As this matrix is orthogonal (see Appendix A), the dimension of the DLA is upper bounded by $\frac{1}{2}d_k(d_k - 1)$.

We can thus compute the DLA corresponding to our circuit ¹ in the subspace of the chosen HW k .

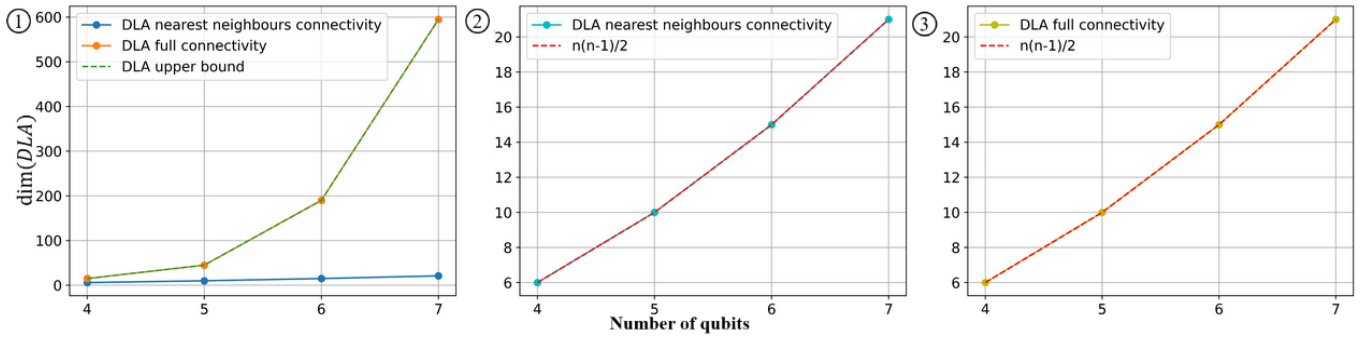


FIG. 3: Evolution of the dimension of the DLA in the subspace of HW $k = \lfloor \frac{n}{2} \rfloor$ for: (1) the use of RBS gates; (2) the use of FBS gates with nearest neighbors connectivity; (3) the use of FBS gates with full connectivity. This plot highlights the difference of controllability potential between RBS and FBS based quantum circuit.

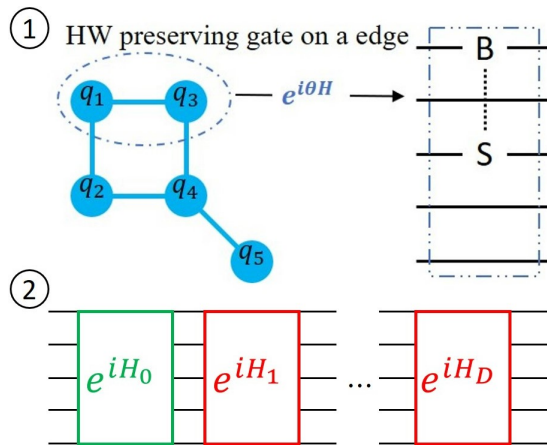


FIG. 4: Hamiltonian representation of a HW preserving VQC: (1) highlights the link between the qubit connectivity and the generators of the circuit, and (2) represents our quantum data loader. The bit flips used to prepare the initial state are represented in green, and RBS are represented red.

If the dimension of the DLA in the subspace of HW k is lower than $d_k - 1$ (with $d_k = \binom{n}{k}$), we cannot control enough coefficients to achieve the encoding described in Eq. (6). If the dimension is maximal (equal to $\frac{1}{2}d_k(d_k - 1)$), we can perfectly control W^k , and thus we can design a loader. Between those two values, we cannot ensure the existence of a loader using the DLA dimension as we may control at least $d_k - 1$ coefficients but not those in the columns corresponding to $|e_s\rangle$. In practice, one could choose to reduce the choice of k to achieve the full controllability of the subspace or could

proceed with our method to find the data loader given in Section II C. Indeed, one can use the rank of the Quantum Fisher Information matrix to ensure this sufficient controllability in the state space (see Section II C).

We know that having enough control to design a quantum data loader requires considering a connected graph in order to reach any state in our encoding basis. Therefore, the nearest neighbor's connectivity is the worst as it has a minimal number of edges, and full connectivity maximizes the dimension of the DLA. The scaling of the DLA dimension according to a specific type of graph needs to be tackled in future work, but Fig. 3 gives numerical evidence of good scaling in terms of controllability for an RBS based quantum circuit.

We observe in the Fig. 3 that the evolution of the DLA dimension in the nearest neighbors connectivity setting seems to follow the maximum controllability of the first subspace, which is given by $\frac{1}{2}n(n-1)$. The DLA dimension for the maximum connectivity seems to evolve according to the upper bound given by the maximum controllability of a $d_{n/2} \times d_{n/2}$ orthogonal matrix and equal to $\frac{1}{2}d_{n/2}(d_{n/2} - 1)$ when considering RBS gates. In the case of the FBS gates, we know that each block W^k is perfectly determined by the first one W^1 [22] (see Appendix C). As a result, the dimension of the DLA of FBS based quantum circuit is upper-bounded by $\frac{1}{2}n(n-1)$ as observed in the previous figure. The limitation of the controllability of FBS gates is reminded in Appendix C.

In this section we show that the DLA study gives us tools to know if we can design a quantum data loader from a qubit connectivity and a specific quantum gate.

C. Finding the quantum data loader

Using previous results, we know that if we have a quantum hardware such that the DLA dimension is high enough, there exists a quantum data loader circuit. A remaining question is how to design the quantum data

¹ Hamiltonians in Fig. 4 do not commute, but the Lie Algebra generated by the sum of those Hamiltonians is equal to the one given by the global Hamiltonian according to the Baker-Campbell-Hausdorff formula.

loader from a given subspace and the connectivity that induces the existence of such a circuit. In this Section, we will present two algorithms to design the quantum data loader based on the study of controllability in the state space.

A subspace preserving circuit's ability to achieve amplitude encoding on one of its preserved subspaces is equivalent to saying that this circuit perfectly controls the state space created by its output. In particular, a RBS based VQC can achieve amplitude encoding (see Definition 1) on the subspace of HW k if the output state can be any superposition of states in B_k^n . The state space spanned by the output of the VQC is thus a sphere of dimension $d_k - 1$ noted $S^{d_k - 1}$ and illustrated in Fig. 5.

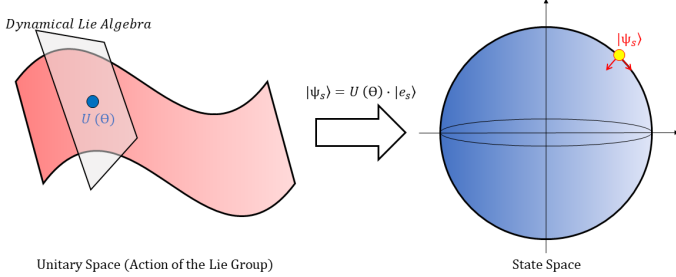


FIG. 5: Representation of the unitary and output state spaces. The DLA is the tangent space of the unitary space. The possible directions for the evolution of the output state are given by the Quantum Fisher Information Matrix eigenvectors.

Now we define an essential tool to study the controllability of a quantum circuit in the state space.

Definition 6 (Quantum Fisher Information Matrix). *Let us consider an initial state $|e_s\rangle$ and $U(\Theta)$ the unitary that represents a quantum circuit with $\Theta = \{\theta_1, \dots, \theta_D\}$ the set of variational parameters. The Quantum Fisher Information Matrix (QFIM) is a $D \times D$ matrix defined as:*

$$[QFIM_s(\Theta)]_{i,j} = 4\text{Re}\left[\langle \partial_{\theta_i} \psi_s(\Theta) | \partial_{\theta_j} \psi_s(\Theta) \rangle - \langle \partial_{\theta_i} \psi_s(\Theta) | \psi_s(\Theta) \rangle \langle \psi_s(\Theta) | \partial_{\theta_j} \psi_s(\Theta) \rangle\right] \quad (10)$$

with $|\psi_s(\Theta)\rangle = U(\Theta) |e_s\rangle$

The maximal rank of the QFIM is a metric of controllability in the state space [25], as it gives us the number of independent directions that can be taken by the state when tuning the gate parameters Θ . For our encoding method in the subspace of HW k , the maximum rank is given by the topology of the sphere $S^{d_k - 1}$:

$$\max_{\Theta} \text{rank}[QFIM_s(\Theta)] \leq d_k - 1 \quad (11)$$

As in [26], we find numerical evidence (see Fig. 6) that:

$$\forall \Theta \in [0, 2\pi]^D \quad \text{rank}[QFIM_s(\Theta)] = \max_{\Theta} \text{rank}[QFIM_s(\Theta)] \quad (12)$$

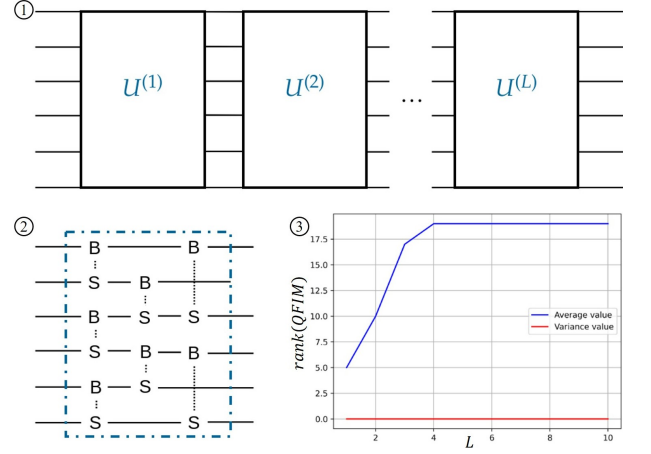


FIG. 6: Evolution of the rank of the QFIM for a periodic structure ansatz presented in (1). Each block is represented in (2), and the evolution of the rank of the corresponding QFIM is given by (3). The derivation of the QFIM rank is done in the largest subspace ($k = n/2 = 3$).

By property of the orthogonal group, we know that the unit sphere is a homogeneous space of the action of the Lie Group that is described by our encoding method. As a result, we can state the following lemma:

Lemma 1. *Let us consider the subspace of HW k of our n -qubits encoding method. If the rank of the QFIM in the subspace is maximal on one point:*

$$\exists \Theta \in [0, 2\pi]^D \mid \text{rank}[QFIM(\Theta)] = d_k - 1 \quad (13)$$

Then:

$$\forall \Theta \in [0, 2\pi]^D, \quad \text{rank}[QFIM(\Theta)] = d_k - 1 \quad (14)$$

Using the QFIM on a given subspace of HW k , we propose a first algorithm to design a quantum data loader in this subspace from an initial state created using bit-flips, and the possible generators \mathcal{G} given by the qubit connectivity and the RBS gate Hamiltonian. When the rank of the QFIM of a quantum data loader circuit is equal to $d_k - 1$, the state space is $S^{d_k - 1}$. It can therefore achieve any superposition of states from B_k^n , i.e., achieve the amplitude encoding on the subspace of HW k . The Algorithm 1 consists in adding RBS gates and measure the new rank of the QFIM, until it achieves its maximal value, ensuring the data loader capability.

Algorithm 1 to design a HW preserving quantum data loader

Require: \mathcal{G} the generators, $|e_s\rangle$ the initial state

- 1: circuit = \emptyset
 - 2: **while** ($\max_{\Theta} \text{rank}[QFIM(\text{circuit}, \Theta)] < d_k - 1$) **do**
 - 3: **for** $RBS \in \mathcal{G}$ **do**
 - 4: circuit' = circuit + RBS
 - 5: **if** ($\max_{\Theta'} \text{rank}[QFIM(\text{circuit}', \Theta')] >$
 $\max_{\Theta} \text{rank}[QFIM(\text{circuit}, \Theta)]$) **then**
 - 6: circuit = circuit'
 - 7: **return** circuit
-

Using the conjecture given by Eq.(12), we can only consider one point of the state space to derive the maximum rank of the QFIM. To avoid this conjecture, we propose the Algorithm 2, using overparametrization, a concept introduced in [11]:

Definition 7 (Overparametrization). *A VQC overparametrized if the number of parameters D is such that the QFIM, for all the states in the training set, simultaneously saturate their rank R_s :*

$$\max_{D \geq D_c, \Theta} \text{rank}[QFIM_s(\Theta)] = R_s \quad (15)$$

The authors showed that for a general type of periodic-structured VQCs, we have:

$$D_c \sim \text{dim}(DLA) \quad (16)$$

The quantum circuit that performs the full rank of the QFIM can be easily completed using overparametrization according to Eq.(16). Using Theorem 1, we know that we only need to derive the rank of the QFIM on a single point to find its maximal value.

Algorithm 2 to design a HW preserving quantum data loader

```

Ensure: circuit, flag = True
1: while flag do
2:   flag = False
3:   for  $RBS \in$  circuit do
4:     circuit' = circuit -  $RBS$ 
5:     if  $(\max_{\Theta'} \text{rank}[QFIM(\text{circuit}', \Theta')]) =$ 
        $\max_{\Theta} \text{rank}[QFIM(\text{circuit}, \Theta)]$  then
6:       circuit, flag = circuit', True
7:     break for
8: return circuit

```

The reason we can naively increase the rank of the QFIM to its maximal in Algorithm 1 is because of the results from [11] on the Theory of Overparametrization, reminded in Definition 7. In practice, Algorithm 2 is initialized by considering a quantum circuit made of a high number of gates according to the dimension of its DLA as explained in Eq.(16). Those gates can be chosen randomly or in such a way to reduce the circuit depth.

In practice and with both algorithms, one must pay particular attention to the order of the generators that are tested in the algorithm with regard to the circuit depth.

III. TRAINABILITY OF HW PRESERVING QUANTUM CIRCUITS

In the previous Section, we discussed how to prove the existence of a quantum data loader using RBS gates and how to design such an encoding circuit for a specific subspace. In this Section, we show a study of the trainability of HW preserving quantum circuits that could be used

for our encoding but also for other types of trainable layers, such as represented in Fig. 1. It is known that some QML proposals suffer from negative optimization landscape properties [10] that lead to strong limitation in their trainability. In this Section, we will give strong results on the gradient of the cost function for VQC made of RBS or FBS gates. First, we present in Section III A the backpropagation formalism applied to RBS and FBS based VQC. Then we present the resulting theorems on the variance and expectation value of the cost function gradient in Section III B.

A. Backpropagation for gradient calculus

We describe a HW preserving quantum circuit only made of RBS gates. We decompose the quantum circuit as a set of λ_{max} gates. At each time step λ , we call the inner layers ζ^λ the quantum states in the circuit, and the inner errors $\delta^\lambda = \partial \mathcal{C} / \partial \zeta^\lambda$. We call w^λ the unitary in the considered basis B_k^n for each RBS. The cost function is $\mathcal{C}(\Theta) = \|z - y\|_2^2$ with z the output of the quantum circuit, and y the desired output.

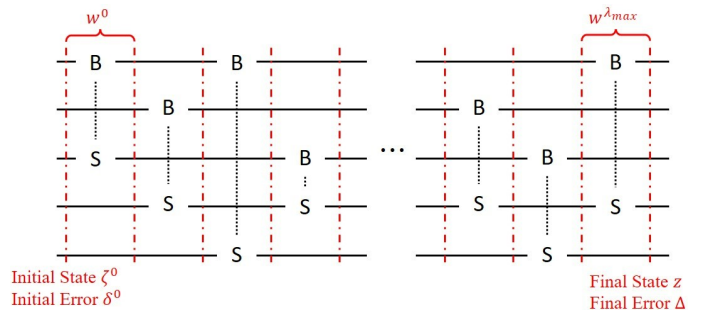


FIG. 7: Decomposition of the HW preserving quantum circuit for the backpropagation method.

The equivalent weight matrix of our VQC is $W^k = w^{\lambda_{max}} \dots w^1 w^0$. To train our circuit, we want to update each RBS parameter θ_i with respect to the gradient of the cost function \mathcal{C} . We derive the gradient by decomposing it using each component, indexed by the integer p , of the inner layer and inner error vectors:

$$\frac{\partial \mathcal{C}}{\partial \theta_i} = \sum_p \frac{\partial \mathcal{C}}{\partial \zeta_p^{\lambda+1}} \frac{\partial \zeta_p^{\lambda+1}}{\partial \theta_i} = \sum_p \delta_p^{\lambda+1} \frac{\partial (w_p^\lambda \cdot \zeta^\lambda)}{\partial \theta_i} \quad (17)$$

Each parameter θ_i corresponds to applying a θ_i -planar rotation between two qubits. We call (l, j) the tuples of states affected by the rotation. Using RBS gates, it comes to:

$$\frac{\partial \mathcal{C}}{\partial \theta_i} = \sum_{(l,j)} \delta_l^\lambda (-\sin(\theta_i) \zeta_l^\lambda + \cos(\theta_i) \zeta_j^\lambda) + \delta_j^\lambda (-\cos(\theta_i) \zeta_l^\lambda - \sin(\theta_i) \zeta_j^\lambda) \quad (18)$$

One can decompose the same way a FBS based quantum circuit in a specific subspace of a given HW:

$$\begin{aligned} \frac{\partial \mathcal{C}}{\partial \theta_i} = & \sum_{(l,j)} \delta_l^\lambda [-\sin(\theta_i)\zeta_l^\lambda + (-1)^{f(a,b,\zeta_j^\lambda)} \cos(\theta_i)\zeta_j^\lambda] + \\ & \delta_j^\lambda ((-1)^{f(a,b,\zeta_l^\lambda)+1} \cos(\theta_i)\zeta_l^\lambda - \sin(\theta_i)\zeta_j^\lambda) \end{aligned} \quad (19)$$

With $f(a,b,\zeta_i^\lambda) = \sum_{a < p < b} s_p$ where $s \in \{0,1\}^n$ is the binary word corresponding to the state given by the index i : $|\zeta_i^\lambda\rangle = |s_1 \cdots s_n\rangle$ (a and b are the qubits affected by the FBS).

B. Avoiding Barren Plateaus

We can use the backpropagation analytic definition of the cost function gradient to study the phenomenon of Barren Plateaus, where certain circumstances lead to exponentially vanishing gradients.

Definition 8 (Barren Plateau). *The cost function $\mathcal{C}(\Theta)$ landscape of a n -qubit VQC is said to exhibit a Barren Plateau (BP) if:*

$$\forall \theta_i \in \Theta, \quad \mathbb{E}_\Theta[\partial_{\theta_i} \mathcal{C}(\Theta)] = 0 \quad \text{and} \quad \text{Var}_\Theta[\partial_{\theta_i} \mathcal{C}(\Theta)] = O\left(\frac{1}{b^n}\right) \quad (20)$$

with $b > 1$

It is possible to determine the existence of BP under the hypothesis of approximate 2-design. This allows to derive the value of $\text{Var}_\Theta[\partial_{\theta_i} \mathcal{C}(\Theta)]$ using the integration formulas from [27]. This results in an expression of the variance inverse of the size of the Hilbert space. In recent work [28], authors have shown under this hypothesis, and the hypothesis of full controllability of the subspace (meaning that the dimension of the DLA is maximal), that using a subspace invariant quantum circuit the expression of the variance is inverse of the dimension of the subspace. As a result, one could avoid BP using a subspace invariant quantum circuit with a subspace of small dimension.

In the following, we will show that one could avoid BP for subspace invariant quantum circuits based on RBS or FBS gates by choosing any subspace of HW k with a fixed k without considering the 2-design hypothesis and with any controllability.

Theorem 1 (Evolution of the variance for RBS and FBS based quantum circuits). *Let us consider a n -qubit HW preserving VQC made of RBS or FBS gates. We consider here the subspace of HW k , i.e., corresponding to the basis B_k^n . If the initial state and the wanted output are Haar distributed on the basis B_k^n , we have that:*

$$\mathbb{E}_\Theta[\partial_{\theta_i} \mathcal{C}(\Theta)] = 0, \quad \text{Var}_\Theta[\partial_{\theta_i} \mathcal{C}(\Theta)] \approx \frac{k(n-k)}{n(n-1)} \frac{8}{d_k} \quad (21)$$

for any $\theta_i \in \{\theta_1, \dots, \theta_D\}$, and with $d_k = \binom{n}{k}$.

The complete proof of this Theorem is presented in Appendix D. We use the hypothesis that the input and the desired output of the RBS quantum circuit are Haar distributed on the considered state basis. This hypothesis might not be verified in all cases. In the encoding use case, we may consider a Haar distributed wanted output but a single input state. In the case of a trainable layer made of RBS or FBS gates (see Appendix IV D) we may consider Haar distributed input, but the desired output may be very concentrated. We illustrate this result in Fig. 9 in the additional simulations given in Appendix IV.

Theorem 2 (Evolution of the variance for RBS and FBS based quantum data loader). *Let us consider a n -qubit HW preserving VQC made of RBS or FBS gate. We consider here the subspace of HW k , i.e. corresponding to the basis B_k^n . If the initial state is a single state $|e_s\rangle \in B_k^n$ and the wanted output is Haar distributed on the basis B_k^n , we have that:*

$$\forall i \geq \lambda_0, \quad \mathbb{E}_\Theta[\partial_{\theta_i} \mathcal{C}(\Theta)] = 0, \quad \text{Var}_\Theta[\partial_{\theta_i} \mathcal{C}(\Theta)] \approx \frac{k(n-k)}{n(n-1)} \frac{8}{d_k} \quad (22)$$

with λ_0 is such that from the gate with variational parameter θ_{λ_0} every state in B_k^n can be reached. We recall that $d_k = \binom{n}{k}$.

The complete proof of this Theorem is presented in Appendix E. After a certain number of gates λ_0 , the expectation value is uniformly spread on the basis states, which is very similar to the situation of Theorem 1. The same Theorem could be stated for the case where the desired output is included in a restricted number of states and the input is Haar distributed on the basis B_k^n , corresponding to the use of a VQC in a subspace of HW k as a neural network. We illustrate this result in Fig. 10 in the additional simulations given in Appendix IV.

We can conclude from these results that there is no Barren Plateaus for the subspace invariant RBS and FBS based quantum circuits for a fixed choice of subspace k according to the scaling of d_k , the dimension of the subspace of HW k .

C. Complexity and simulation of subspace preserving RBS circuit

According to its better controllability properties, we focus on RBS gates. In the subspace of HW k , the effect of a RBS gate is a rotation between k couples of states in the basis B_k^n . Therefore, a RBS is easy to simulate classically in the unary basis but requires an exponential number of operations when k is close to $n/2$ as $d_{n/2}$ grows exponentially with n the number of qubits. Nevertheless, using a greater subspace may be a wrong choice according to the circuit depth. For example, achieving the full controllability of a larger subspace requires a more significant amount of gates but the number of qubits is limited.

It results in a rise in the circuit depth. In addition, using a greater subspace results in the apparition of BP, as shown in III.

Algorithm	Feedforward	Training
Quantum RBS VQCs	$\mathcal{O}(D/(p * \delta^2))$	$\mathcal{O}((D/p)^2)$
Classical RBS VQCs	$\mathcal{O}(D \binom{n-2}{k-1})$	$\mathcal{O}((D \binom{n-2}{k-1})^2)$

TABLE I: Running time summary. n is the number of qubits, k the chosen Hamming weight corresponding to the selected subspace, and δ is the error parameter in the quantum implementation. We call p the average number of gates we can parallelize at the same time (upper-bounded by $\lfloor \frac{n}{2} \rfloor$).

However, the use of subspace preserving RBS quantum circuits is keen on giving a speedup advantage for an application that requires to proceed a large amount of information but with a limited number of degrees of freedom (and thus of RBS gates). In Section IV D, we give an example of such an application for a fully connected orthogonal neural network that is not fully controllable. Problem-inspired architectures using symmetries are perfect candidates for this type of application.

IV. ADDITIONAL SIMULATIONS

In this section, we present additional simulations. We propose to illustrate the use of Algorithm 1 for an existing hardware and the corresponding simulations in Section IV A. In Section IV B, we propose additional simulations to illustrate the results in Section III.

A. Using our encoding method for an existing hardware

In this part, we propose to use the Algorithm 1 to design a 5-qubit quantum data loader that fits the Rigetti ASPEN M2 connectivity given in Fig. 8. This hardware is keen on implementing such a data loader thanks to its high connectivity and to the fact that the RBS gate is native to this platform (and called the XY gate).

Using the Algorithm 1, we can design a quantum data loader for this connectivity. To minimize the depth, one can use in practice a variation of this algorithm that minimizes the depth by testing in priority the gates that are more likely to parallelize themselves. As a result, the circuit obtained is given in Fig. 8.

In order to highlight the performance of our quantum data loader, we simulate our method using python numpy but also using Qiskit, a quantum instruction language developed as a python library by IBM. We test our data loader for a well-known data set called the Fashion MNIST dataset.

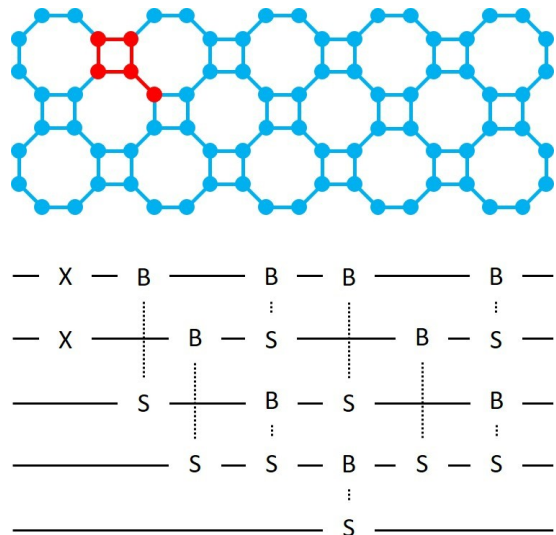


FIG. 8: Rigetti ASPEN M2 connectivity graph and the Quantum Data loader quantum circuit obtained using our Algorithm 1.

Simulation tool used	Average Error	Error Variance
Numpy	0.0097	0.00030
Qiskit	0.0094	0.00028

TABLE II: Performance of the quantum data loader presented in Fig. 8.

To achieve this simulation, we use our codes after applying a Principal Component Analysis (PCA) to reduce our dataset to $\binom{n}{k}$ -dimensional vector, with $n = 5$ the number of qubits, and $k = 2$ the chosen HW. We used 1000 samples to derive those values.

The approximation error is measured using the following cost function between the real state that we are supposed to have x^* and the output of our quantum system given by $x = W^k(\theta) \cdot e_s$ (with e_s the vector representation of the initial state in our method):

$$\mathcal{C}(x) = \|W^k(\Theta) \cdot e_s - x^*\|_2^2 \quad (23)$$

For an actual implementation on a Quantum Processor Unit, one can generalize the tomography procedure described in [6].

B. Trainability of Hamming weight preserving quantum circuits

In this part, we illustrate the results obtained from section III on the trainability of RBS and FBS gate based quantum circuits in a specific subspace corresponding of a choice of Hamming weight k .

In Fig. 9, we plot the average value and the variance of the gradient for quantum circuits made only of RBS

and FBS with a random choice of parameters, input, and target output. This setting corresponds to the case of Theorem 1. We observe that the average gradient is close to zero and its variance corresponds to the theoretical values. In Theorem 1, the result is an average for a Haar distributed inputs and the target outputs. In our simulation, we choose to plot the study of the cost function while choosing randomly the inputs, and the target outputs. To do so, we considered those states as $\binom{n}{k}$ -dimensional vectors with coefficients uniformly distributed in $[-1, 1]$, and we normalized them afterwards. As a result, the distribution of the input and target states are not exactly Haar distributed.

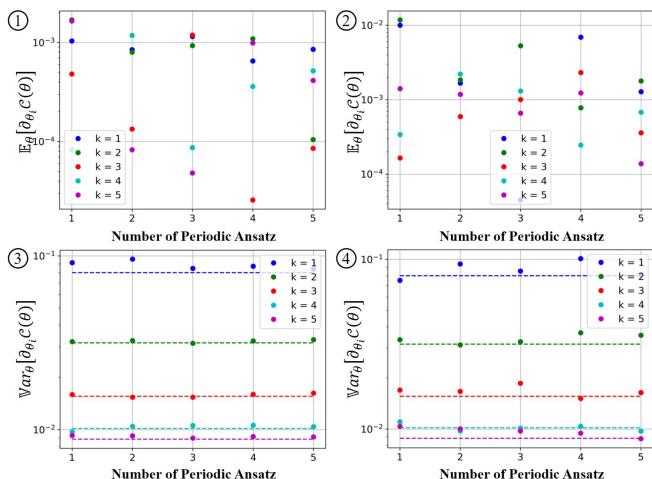


FIG. 9: Gradient study for the same Periodic Structure Ansatz as in Fig. 6. Using 100 random choices of input, wanted output, and parameters, we plot the average value of the gradient for each number of periodic ansatz L in (1). In (2), we plot the average gradient in the case where the RBS are replaced by FBS. In (3), we derive the variance of the gradient for the RBS case, and in (4), the variance for the FBS case. The dotted lines correspond to the theoretical values from Theorem 1.

In the previous Figure, one can notice that the value of the variance of the gradient is unchanged with the number of periodic ansatz L . As the number of periodic ansatz increase, the number of gates increase but also the controllability in the state space. Indeed, Fig. 6 shows the evolution of the controllability in the state space by presenting the evolution of the QFIM rank with L (the maximal controllability is achieved with $L = 4$). Therefore, Fig. 9 highlights a in-dependency between the controllability in the state space and the trainability.

In Fig. 10, we plot the average value and the variance of the gradient for quantum circuits made only of RBS and FBS with a random choice of parameters and target output. We fix the choice of the input state to be the initial state where the k first qubits are initialized in state $|1\rangle$. This setting corresponds to the case of Theorem 2, very similar to the case of our encoding described

in Section II. This is the reason why the variance of the gradient is null for some of the first gates that don't affect the initial state.

The theoretical variance values in this Theorem is stated for the parameters corresponding to the gates after a certain rank λ_0 . According to the subspace choice k , the rank λ_0 represents the number of gates necessary to reach any states in the state basis B_k^n . Therefore, we can see in Fig. 10 that the first points for any subspace k are quite far from the theoretical values, but as the number of the gate increases, the points get closer to our theoretical results.

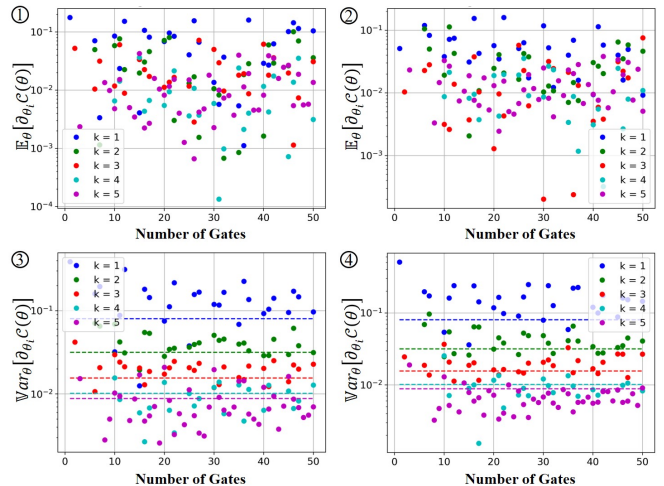


FIG. 10: Gradient study for a quantum circuit made of 5 consecutive block circuits as described in Fig. 6. The plots are numerical evidences of Theorem 2 as the expectation values of the gradient are close to 0 and the variances follow the theoretical values given by the dotted lines. The initial state is fixed as a single state in B_k^n for any subspace choice k . We use 10000 random target output and set of parameters.

C. HW preserving VQC for Neural Networks

In our work, we introduce an encoding method using subspace invariant quantum circuits with a focus on the HW preserving systems, the RBS, and the FBS gates. In this particular setting, the capacity of classically simulate such a circuit is not an issue as one may use our encoding method with an additional circuit hard to classically simulate. However, the results given in section III highlights the interest of using such circuit as neural networks. In addition, the use of Hamming weigh preserving quantum circuits for machine learning purposes has already been proposed in [5–7, 22], and we could generalize those methods for larger subspace with better speedups.

In this Section, we present how to use our results for Neural Networks. First, we introduce in III C the complexity of a RBS based quantum circuit. Then we present

in [IV D](#) the use of a RBS based VQC for image classification for a toy example.

D. RBS based Quantum Orthogonal Neural Network

In this section, we illustrate the fact that we can use our results for Quantum Neural Network (QNN) application. In particular, one can consider a RBS circuit in a particular HW basis B_k^n in order to design an orthogonal neural network, as the equivalent unitary in the corresponding Hilbert space $W^k(\Theta)$ is orthogonal according to [Theorem 3](#). In [Fig. 11](#), we plot the training and the testing accuracy for binary classification on the Fashion MNIST dataset where we use the quantum circuit described in [Fig. 8](#) as a QNN.

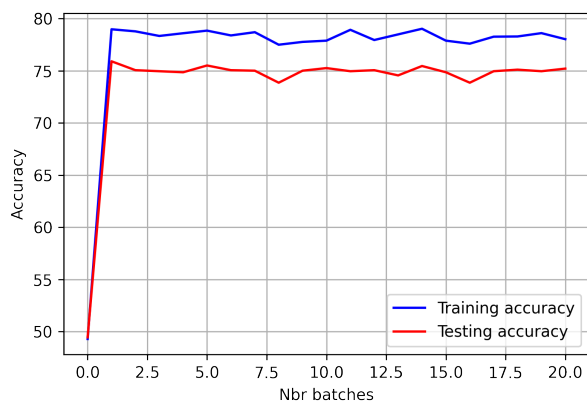


FIG. 11: Binary classification on the Fashion MNIST data set for 10000 training samples and 5000 testing samples. The optimization method is ADAM with a batch size of 5, and we used is the Cross Entropy Cost.

We do not claim that this plot exhibits any advantage to use RBS based quantum circuits as neural networks, but it illustrates that we can easily use such an architecture. The fact that the testing accuracy is higher than the training one v Large simulation for more complex HW preserving quantum neural networks for large value of k must be tackled in future work.

According to the complexity of such RBS models described in [Table I](#), there is no exponential advantage in using a quantum orthogonal neural network. In [\[6\]](#), the authors present the use of a specific case of such a RBS model in the unary basis and show a quadratic advantage for a fully controllable QNN in the unary basis called the Pyramidal Quantum Neural Network (PQNN). For specific use cases that require less controllability but higher-dimensional input data, one can prefer to use a RBS based orthogonal neural network in a larger Hamming weight basis and can achieve a more significant speedup.

V. DISCUSSION

In this work, we study the controllability and the trainability of a subspace-preserving variational quantum circuit through the prism of designing a quantum data loader using RBS gates. We show that the encoding capacity is linked with the controllability of the quantum system and that using only a certain type of gates, the controllability is linked with the connectivity of the hardware. In addition, we show how to study mathematical tools such as the Dynamical Lie Algebra or the Quantum Fisher Information Matrix in order to design a data loader. Finally, we show how to avoid Barren Plateaus for variational quantum circuits only made of RBS or FBS gates.

The results we show for the trainability of Hamming weight preserving quantum circuits must be compared with our results on the controllability. Indeed, it is now clear that there is a trade-off between the expressivity of a variational quantum circuit and its trainability. In recent work [\[11\]](#), authors have shown the connection between the dimension of the Dynamical Lie Algebra (DLA) and the gradient variance of subspace preserving variational quantum circuit in the specific setting of the subspace full controllability and with a 2-design hypothesis on the used ansatz. As a result, they show that such gradient variance evolves in an inverse manner with the dimension of the DLA. They also left open [Conjecture 1](#). More recently, [\[17\]](#) and [\[18\]](#) have shown that this evolution is true in a more general setting and hence proved the [Conjecture 1](#) to be true, under some assumptions on the initial state and the observable. In [\[18\]](#), the authors also claim that RBS and FBS based quantum circuits are not part of their framework and show a coherent result to ours by given an upper-bound on the abstract variance of such circuit. Our results are independent from those papers, and show theoretical guarantees for RBS and FBS based VQC in a general setting.

Conjecture 1 (from [\[11\]](#)). *Let the state ρ belong to a subspace \mathcal{H}_k associated with a subspace DLA \mathfrak{g}_k (or sub-DLA, the subrepresentation in \mathfrak{g} where ρ has support on). Then, the scaling of the cost function partial derivative is inversely proportional to the scaling of the dimension of the DLA, i.e.*

$$\text{Var}_{\Theta}[\partial_{\mu}\mathcal{C}(\Theta)] \in \mathcal{O}\left(\frac{1}{\text{poly}(\dim(\mathfrak{g}_k))}\right) \quad (24)$$

In our work, we show that for the specific cases of RBS/FBS circuits and preserved subspace based on Hamming weight, the cost gradient variance evolves in an inverse manner with the dimension d_k of the subspace, and not as stated in [Conjecture 1](#). In general, it is very hard to compute the expectation value and the variance of a subspace preserving variational circuit gradient. The use of the 2-design hypothesis gives tools to study the gradient [\[27\]](#) but is a huge hypothesis on the expressivity of the quantum system that often leads to

considering that the system is fully controllable. In the specific case of RBS and FBS gates, the expressions of those gates are easy to manipulate analytically, and we are able to prevent the use of use hypothesis.

Although our work give theoretical guarantees on the trainability of a specific type of VQC, we show that those methods could be useful for near term QML. In addition, we would like to insist on the fact that one cannot state in general that the trainability of a VQC is perfectly defined by its controlability through the dimension of the corresponding DLA. First because the dimension of the DLA is only an upper-bound on the controlability, but also because we show an example of a VQC where the previous conjecture from [11] is refuted. In our setting, only the dimension of the subspace is involved in the scaling of the cost gradient variance. Therefore, one needs to be careful to consider the smallest subspace possible. For example, if you consider a RBS based quantum circuit but where some states in B_k^n cannot be reached, you may need to

consider a new smaller subspace more appropriate.

VI. ACKNOWLEDGMENT

This work is also supported by the H2020-FETOPEN Grant PHOQUSING (GA no.: 899544), the Engineering and Physical Sciences Research Council (grants EP/T001062/1), and the Naval Group Centre of Excellence for Information Human factors and Signature Management (CEMIS). ABG is supported by ANR JCJC TCS-NISQ ANR-22-CE47-0004, and by the PEPR integrated project EPiQ ANR-22-PETQ-0007 part of Plan France 2030. This work is part of HQI initiative (www.hqi.fr) and is supported by France 2030 under the French National Research Agency award number ANR-22-PNCQ-0002.

-
- [1] M. Cerezo, A. Arrasmith, R. Babbush, S. C. Benjamin, S. Endo, K. Fujii, J. R. McClean, K. Mitarai, X. Yuan, L. Cincio, and P. J. Coles, (2020), [10.1038/s42254-021-00348-9](https://arxiv.org/abs/10.1038/s42254-021-00348-9), [arXiv:2012.09265](https://arxiv.org/abs/2012.09265).
- [2] A. W. Harrow, A. Hassidim, and S. Lloyd, (2008), [10.1103/PhysRevLett.103.150502](https://arxiv.org/abs/10.1103/PhysRevLett.103.150502), [arXiv:0811.3171](https://arxiv.org/abs/0811.3171).
- [3] I. Kerenidis and J. Landman, (2020), [10.1103/PhysRevA.103.042415](https://arxiv.org/abs/10.1103/PhysRevA.103.042415), [arXiv:2007.00280](https://arxiv.org/abs/2007.00280).
- [4] S. Lloyd, M. Mohseni, and P. Rebentrost, (2013), [10.1038/nphys3029](https://arxiv.org/abs/10.1038/nphys3029), [arXiv:1307.0401](https://arxiv.org/abs/1307.0401).
- [5] S. Johri, S. Debnath, A. Mocherla, A. Singh, A. Prakash, J. Kim, and I. Kerenidis, (2020), [arXiv:2012.04145](https://arxiv.org/abs/2012.04145).
- [6] J. Landman, N. Mathur, Y. Y. Li, M. Strahm, S. Kazdaghli, A. Prakash, and I. Kerenidis, (2022), [10.22331/q-2022-12-22-881](https://arxiv.org/abs/10.22331/q-2022-12-22-881), [arXiv:2212.07389](https://arxiv.org/abs/2212.07389).
- [7] E. A. Cherrat, I. Kerenidis, N. Mathur, J. Landman, M. Strahm, and Y. Y. Li, (2022), [arXiv:2209.08167](https://arxiv.org/abs/2209.08167).
- [8] M. Schuld, R. Sweke, and J. J. Meyer, (2020), [10.1103/PhysRevA.103.032430](https://arxiv.org/abs/10.1103/PhysRevA.103.032430), [arXiv:2008.08605](https://arxiv.org/abs/2008.08605).
- [9] J. Landman, S. Thabet, C. Dalyac, H. Mhiri, and E. Kashefi, (2022), [arXiv:2210.13200](https://arxiv.org/abs/2210.13200).
- [10] J. R. McClean, S. Boixo, V. N. Smelyanskiy, R. Babbush, and H. Neven, (2018), [10.1038/s41467-018-07090-4](https://arxiv.org/abs/10.1038/s41467-018-07090-4), [arXiv:1803.11173](https://arxiv.org/abs/1803.11173).
- [11] M. Larocca, P. Czarnik, K. Sharma, G. Muraleedharan, P. J. Coles, and M. Cerezo, (2021), [10.22331/q-2022-09-29-824](https://arxiv.org/abs/10.22331/q-2022-09-29-824), [arXiv:2105.14377](https://arxiv.org/abs/2105.14377).
- [12] M. Larocca, F. Sauvage, F. M. Sbah, G. Verdon, P. J. Coles, and M. Cerezo, (2022), [10.1103/PRXQuantum.3.030341](https://arxiv.org/abs/10.1103/PRXQuantum.3.030341), [arXiv:2205.02261](https://arxiv.org/abs/2205.02261).
- [13] J. J. Meyer, M. Mularski, E. Gil-Fuster, A. A. Mele, F. Arzani, A. Wilms, and J. Eisert, (2022), [10.1103/PRXQuantum.4.010328](https://arxiv.org/abs/10.1103/PRXQuantum.4.010328), [arXiv:2205.06217](https://arxiv.org/abs/2205.06217).
- [14] T. S. Cohen and M. Welling, (2016), [arXiv:1602.07576](https://arxiv.org/abs/1602.07576).
- [15] X. You, S. Chakrabarti, and X. Wu, “A convergence theory for over-parameterized variational quantum eigensolvers,” (2022), [arXiv:2205.12481](https://arxiv.org/abs/2205.12481).
- [16] E. R. Anschuetz and B. T. Kiani, (2022), [10.1038/s41467-022-35364-5](https://arxiv.org/abs/10.1038/s41467-022-35364-5), [arXiv:2205.05786](https://arxiv.org/abs/2205.05786).
- [17] M. Ragone, B. N. Bakalov, F. Sauvage, A. F. Kemper, C. O. Marrero, M. Larocca, and M. Cerezo, “A unified theory of barren plateaus for deep parametrized quantum circuits,” (2023), [arXiv:2309.09342](https://arxiv.org/abs/2309.09342).
- [18] E. Fontana, D. Herman, S. Chakrabarti, N. Kumar, R. Yalovetzky, J. Heredge, S. H. Sureshbabu, and M. Pistola, “The adjoint is all you need: Characterizing barren plateaus in quantum ansätze,” (2023), [arXiv:2309.07902](https://arxiv.org/abs/2309.07902).
- [19] D. Wecker, M. B. Hastings, and M. Troyer, (2015), [10.1103/PhysRevA.92.042303](https://arxiv.org/abs/10.1103/PhysRevA.92.042303), [arXiv:1507.08969](https://arxiv.org/abs/1507.08969).
- [20] E. Farhi, J. Goldstone, and S. Gutmann, “A quantum approximate optimization algorithm,” (2014), [arXiv:1411.4028](https://arxiv.org/abs/1411.4028).
- [21] S. Hadfield, Z. Wang, B. O’Gorman, E. G. Rieffel, D. Venturelli, and R. Biswas, (2017), [10.3390/a12020034](https://arxiv.org/abs/10.3390/a12020034), [arXiv:1709.03489](https://arxiv.org/abs/1709.03489).
- [22] I. Kerenidis and A. Prakash, (2022), [arXiv:2202.00054](https://arxiv.org/abs/2202.00054).
- [23] M. Cerezo, A. Sone, T. Volkoff, L. Cincio, and P. J. Coles, (2020), [10.1038/s41467-021-21728-w](https://arxiv.org/abs/10.1038/s41467-021-21728-w), [arXiv:2001.00550](https://arxiv.org/abs/2001.00550).
- [24] E. R. Anschuetz, A. Bauer, B. T. Kiani, and S. Lloyd, (2022), [arXiv:2211.16998](https://arxiv.org/abs/2211.16998).
- [25] J. Liu, H. Yuan, X.-M. Lu, and X. Wang, (2019), [10.1088/1751-8121/ab5d4d](https://arxiv.org/abs/10.1088/1751-8121/ab5d4d), [arXiv:1907.08037](https://arxiv.org/abs/1907.08037).
- [26] T. Haug, K. Bharti, and M. S. Kim, (2021), [10.1103/PRXQuantum.2.040309](https://arxiv.org/abs/10.1103/PRXQuantum.2.040309), [arXiv:2102.01659](https://arxiv.org/abs/2102.01659).
- [27] Z. Puchala and J. A. Miszczak, (2011), [10.1515/bpasts-2017-0003](https://arxiv.org/abs/10.1515/bpasts-2017-0003), [arXiv:1109.4244](https://arxiv.org/abs/1109.4244).
- [28] M. Larocca, N. Ju, D. García-Martín, P. J. Coles, and M. Cerezo, (2021), [arXiv:2109.11676](https://arxiv.org/abs/2109.11676).
- [29] J.-C. Faugère, P. Gianni, D. Lazard, and T. Mora, (1993).
- [30] J.-C. Faugère, M. S. E. Din, and P.-J. Spaenlehauer, (1999).
- [31] S. G. Schirmer, H. Fu, and A. I. Solomon, (2000), [10.1103/PhysRevA.63.063410](https://arxiv.org/abs/10.1103/PhysRevA.63.063410), [arXiv:quant-ph/0010031](https://arxiv.org/abs/quant-ph/0010031).

Appendix A: Properties of the RBS gate

In this section, we discuss the properties of the RBS gate. In particular, we first show in A1 that any RBS based quantum circuit can be expressed in the subspace of states of HW k , i.e in the state basis B_k^n , as an orthogonal matrix. Then, we study in A2 the difficulty to find the good set of variational parameters to perform the data loading as expressed in Eq.(6)

1. Orthogonality of RBS equivalent matrix

Theorem 3. *Let us consider $\tilde{W}(\Theta) = (\tilde{w}_{i,j}(\Theta))_{i,j \in [2^n]}$ the unitary matrix corresponding to a quantum circuit only made of RBS gates. We call $W^k(\Theta) = (w_{i,j}(\Theta))_{i,j \in B_k^n}$ the $\binom{n}{k} \times \binom{n}{k}$ equivalent matrix in the basis B_k^n . The matrix $W^k(\Theta)$ is orthogonal.*

Proof of Theorem 3:

We call $v_i \in \mathbb{R}^{\binom{n}{k}}$ the i^{th} column of $W^k(\Theta)$ and $\tilde{v}_i \in \mathbb{R}^{2^n}$ the i^{th} column of $\tilde{W}(\Theta)$. The orthonormality of $W^k(\Theta)$ is given by property on the probability (from each state of the basis, the sum of the probabilities to reach the other states is equal to one) and by property on the unitaries:

$$\forall i, \quad \langle v_i | v_i \rangle = 1 \quad (\text{A1})$$

To show the orthogonality of the equivalent matrix $W^k(\Theta)$, we need to consider the link between its unitary $\tilde{W}(\Theta)$:

$$\forall (i, j) \in B_k^n, \quad \tilde{w}_{i,j}(\Theta) = w_{i,j}(\Theta) \quad (\text{A2})$$

By property on unitaries:

$$\forall (i, j) \in B_k^n \mid i \neq j, \quad \langle \tilde{v}_i | \tilde{v}_j \rangle = \sum_{l=0}^{2^n-1} \tilde{w}_{i,l}(\Theta) \tilde{w}_{l,j}(\Theta) = 0 \quad (\text{A3})$$

RBS gates maintain the Hamming weight of the states:

$$\forall i \in B_k^n, \forall j \notin B_k^n, \quad \tilde{w}_{i,j}(\Theta) = 0 \quad (\text{A4})$$

Thus,

$$\forall (i, j) \in B_k^n \mid i \neq j, \quad \langle \tilde{v}_i | \tilde{v}_j \rangle = \sum_{l \in B_k^n} w_{i,l}(\Theta) w_{l,j}(\Theta) = 0 \quad (\text{A5})$$

Finally,

$$\forall (i, j) \in B_k^n \mid i \neq j, \quad \langle v_i | v_j \rangle = 0 \quad (\text{orthogonality}) \quad (\text{A6})$$

2. Quantum Data Loading equation

We expressed in Eq.(6) the equation that we need to solve to perform the amplitude encoding of $x \in \mathbb{R}^{d_k}$ on the basis B_k^n of states of Hamming weight k . Notice that we express this problem in the subspace of HW k , which means that we only consider on the states in B_k^n . We can express this encoding equation as the following set of equations (here, we suppose that the classical vector has been normalized):

$$\begin{cases} w_{s,1}(\Theta) - x_1 = 0 \\ \dots \\ w_{s,\binom{n}{k}}(\Theta) - x_{\binom{n}{k}} = 0 \end{cases} \quad (\text{A7})$$

With $w_{i,j}$ the matrix coefficient from $W^k(\Theta)$ corresponding to the amplitude to go from state $|e_j\rangle$ to $|e_i\rangle$.

In general, finding the solution (or proving the existence of one solution) of a parametric set of non-linear equations is very hard. However, according to the expression of the RBS gate (3), each coefficient $w_{i,j}(\Theta)$ is a sum of product of cosines and sines of the variational parameters. Thus, using the change of variables:

$$\cos(\theta_i) = c_i \quad \text{and} \quad \sin(\theta_i) = s_i \quad (\text{A8})$$

we can express the parametric set of nonlinear equations as a parametric set of polynomial equations:

$$\begin{cases} f_1(c_1, \dots, c_{(k)}, s_1, \dots, s_{(k)}) - x_1 = 0 \\ \dots \\ f_{(k)}^{(n)}(c_1, \dots, c_{(k)}, s_1, \dots, s_{(k)}) - x_{(k)} = 0 \\ c_1^2 + s_1^2 - 1 = 0 \\ \dots \\ c_{(k)}^2 + s_{(k)}^2 - 1 = 0 \end{cases} \quad (\text{A9})$$

Several tools exist to solve such a polynomial system, for example, Gröbner basis [29, 30], but they may come with a very high computational cost. This is reason why we prefer focus on an equivalent optimization problem as defined by Eq (7).

Appendix B: Dynamical Lie Algebra derivation

In this section, we remind the main properties of the Dynamical Lie Algebra (DLA). First, we give a more formal definition of the DLA. Then, we highlight the link between the dimension of the DLA and the dimension of the unitary equivalent manifold to show the link between the DLA and the degrees of freedom introduce in Section II B.

Definition 9 (Dynamical Lie Algebra). *Let us consider the question of controllability for the Schrödinger operator equation in the general form:*

$$\dot{X} = -iH(u)X, \quad X(0) = \mathbb{1}_{d \times d} \quad (\text{B1})$$

The Dynamical Lie algebra is defined as

$$\mathcal{L} = \text{span}_{u \in \mathcal{U}} \{-iH(u)\} \subseteq \mathfrak{su}(d) \quad (\text{B2})$$

The set of reachable states from system (B1) is the connected Lie group associated with the DLA and called Dynamical Lie Group: $\mathcal{R} = e^{\mathcal{L}}$.

In general, the system is said controllable when $\mathcal{L} = \mathfrak{su}(d)$ (we can achieve any equivalent unitary from the system considered), which is in general equivalent to having $\dim(\mathcal{L}) = d^2 - 1$ with d the dimension of the Hilbert space. It tells us that we can choose each coefficient of the equivalent unitary if we respect the condition that the corresponding matrix is unitary.

The Algorithm 3 [31] allows us to compute the rank of the Lie Algebra generated by a control system. Basically, this algorithms derive the dimension of the Lie Algebra by updating a matrix W with potential generators of the Lie Algebra as columns and derive the rank of this matrix after every test to ensure that it increases the dimension of the spanned space.

Algorithm 3 Rank of the Lie Algebra generated by a control system $\{\hat{H}_0, \dots, \hat{H}_M\}$.

Ensure: $W = H_0$

Ensure: $r = \text{rank}(W)$

```

1: for  $m = 1, 2, \dots, M + 1$  do
2:   if  $\text{rank}([W, H_m]) > r$  then
3:     append  $W$  by column vector  $H_m$ 
4:      $r = r + 1$ 

```

Ensure: $r_0 = 0$

Ensure: $r_n = \text{rank}(W)$

```

5: while  $r_n = r_0$  or  $r = N^2$  do
6:   for  $l = r_0 + 1, \dots, r_n$  do
7:     for  $j = 1, \dots, l - 1$  do
8:        $h = [\hat{W}_{i,l}, \hat{W}_{i,j}]$ 
9:       if  $\text{rank}([W, h]) > r$  then
10:        append  $W$  by column vector  $h$ 
11:         $r = r + 1$ 

```

12: $r_0 = r_n$

13: $r_n = \text{rank}(W)$

14: **return** r_n

Appendix C: Properties of the FBS gate

In this section, we remind some of the properties of FBS gates introduced in [22] to show this gate limitation in term of controllability.

According to Definition 4, the application of a FBS between the qubits i and j , $FBS_{i,j}$, acts as $RBS_{i,j}$ if the parity of the qubits 'between' i and j is even, and is the conjugate gate $RBS_{i,j}(-\theta)$ otherwise. The $FBS_{i,j}$ is a non local gate that can be implemented using an RBS gate together with $\mathcal{O}(|i-j|)$ additional two qubit parity gates with a circuit of depth $\mathcal{O}(\log(|i-j|))$.

Although similar to the RBS gate, the FBS is less controllable. As a HW preserving gate, one can express the FBS gate as a block diagonal matrix (see Fig. 2), where each block W^k is an unitary that represents the action of the FBS in the subspace of state of HW k . However, each block W^k for $k > 1$ is perfectly determined by W^1 as it is the k -compound matrix of W^1 . Therefore, the controllability of the FBS unitary is upper-bounded by the controllability of the first block that represents the effect of the gate in the subspace of unitary states, i.e., states of HW 1. In the unitary basis, the FBS is equivalent of the RBS gate. We can thus conclude that the maximal dimension of the DLA for the FBS is $\frac{1}{2}n(n-1)$.

Definition 10 (Compound matrix). *Given a matrix $A \in \mathbb{R}^{n \times n}$, the compound matrix \mathcal{A}^k for $k \in [n]$ is the $\binom{n}{k}$ dimensional matrix with entries $\mathcal{A}_{IJ}^k = \det(A_{IJ})$ where I and J are subsets of rows and columns of A with size k .*

The limitation in its controllability is illustrated in Fig. 3, and prevents the use of FBS for amplitude encoding on a subspace of HW k with $k > 1$. However, FBS can be used to perform Clifford loader, a loader determined on the entire Hilbert space and restricted to the direct sum of subspace produce by the FBS. In [22], algorithms for quantum determinant sampling, singular value estimation for compound matrices, and for Topological data analysis are presented using FBS gates and Clifford loader.

Appendix D: Proof of Theorem 1

We recall the Theorem 1:

Theorem 1 (Evolution of the variance for RBS and FBS based quantum circuits). *Let us consider a n -qubit HW preserving VQC made of RBS or FBS gates. We consider here the subspace of HW k , i.e., corresponding to the basis B_k^n . If the initial state and the wanted output are Haar distributed on the basis B_k^n , we have that:*

$$\mathbb{E}_{\Theta}[\partial_{\theta_i} \mathcal{C}(\Theta)] = 0, \quad \text{Var}_{\Theta}[\partial_{\theta_i} \mathcal{C}(\Theta)] \approx \frac{k(n-k)}{n(n-1)} \frac{8}{d_k} \quad (21)$$

for any $\theta_i \in \{\theta_1, \dots, \theta_D\}$, and with $d_k = \binom{n}{k}$.

To prove this Theorem, we will first consider the unary case in Section D 1, i.e., the case where the states are in B_n^1 . In the unary case, RBS and FBS are equivalent. Then, we will show how to extend our result to any HW k for RBS in Section D 2. Finally, we will explain in Section D 3 how to adapt this result to the FBS case.

1. Unary case

We consider the case of the quadratic cost function. We call Δ^L the final error:

$$\Delta^L = 2(z^L - y) = 2[(w^{\lambda_{max}} \dots w^{\lambda+1}) \cdot w^{\lambda} \cdot \zeta^{\lambda} - y] \quad (D1)$$

We consider the case where for each inner layer, there is only one RBS gate considered. The number of parameters D is equal to the number of inner layers λ_{max} . We call ζ_j the amplitude of the j^{th} state in the state basis considered of ζ . For each inner layer, the action of the gate in the state basis B_1^n results in a rotation of the amplitudes for two states that we call (l, j) :

$$\zeta^{\lambda+1} = \overrightarrow{cst} + (\cos(\theta_i) \cdot \zeta_l^{\lambda} + \sin(\theta_i) \cdot \zeta_j^{\lambda}) |e_l\rangle + (-\sin(\theta_i) \cdot \zeta_l^{\lambda} + \cos(\theta_i) \cdot \zeta_j^{\lambda}) |e_j\rangle \quad (D2)$$

with $\overrightarrow{cst} \cdot |e_j\rangle = \overrightarrow{cst} \cdot |e_l\rangle = 0$

For example, the action of a RBS with parameter θ_i in B_1^n on the two first qubits of a 4-qubit quantum circuit results in the θ_i -planar rotation between the states $|1000\rangle$ and $|0100\rangle$.

We can define the error according to the final error:

$$\delta^{\lambda+1} = (w^{\lambda+1})^{-1} \dots (w^{\lambda_{max}})^{-1} \cdot \Delta^l = 2[w^\lambda \cdot \zeta^\lambda - (w^{\lambda+1})^{-1} \dots (w^{\lambda_{max}})^{-1} \cdot y] \quad (D3)$$

According to Theorem 3: $\forall \lambda, (w^\lambda)^{-1} = (w^\lambda)^t$.

We call: $\tilde{y} = (w^{\lambda+1})^t \dots (w^{\lambda_{max}})^t \cdot y$ and $\Omega = [0 : 2\pi]^D$

We use the notation \tilde{y}_j for the amplitude of the j^{th} state in the state basis considered of \tilde{y} .

According to the backpropagation formalism presented in Section III A, we have in the unary case:

$$\frac{\partial \mathcal{C}}{\partial \theta_i} = \delta_i^\lambda (-\sin(\theta_i) \zeta_i^\lambda + \cos(\theta_i) \zeta_j^\lambda) + \delta_j^\lambda (-\cos(\theta_i) \zeta_i^\lambda - \sin(\theta_i) \zeta_j^\lambda) \quad (D4)$$

Therefore, we can express the variance of the cost function gradient as:

$$\begin{aligned} \text{Var}_\Theta[\partial_{\theta_i} \mathcal{C}(\Theta)] &= \text{Var}_\Theta[\delta_i^\lambda (-\sin(\theta_i) \zeta_i^\lambda + \cos(\theta_i) \zeta_j^\lambda) + \delta_j^\lambda (-\cos(\theta_i) \zeta_i^\lambda - \sin(\theta_i) \zeta_j^\lambda)] \\ &= \text{Var}_\Theta[\delta_i^\lambda (-\sin(\theta_i) \zeta_i^\lambda + \cos(\theta_i) \zeta_j^\lambda)] + \text{Var}_\Theta[\delta_j^\lambda (-\cos(\theta_i) \zeta_i^\lambda - \sin(\theta_i) \zeta_j^\lambda)] \\ &\quad + 2 \cdot \text{Cov}_\Theta[\delta_i^\lambda (-\sin(\theta_i) \zeta_i^\lambda + \cos(\theta_i) \zeta_j^\lambda); \delta_j^\lambda (-\cos(\theta_i) \zeta_i^\lambda - \sin(\theta_i) \zeta_j^\lambda)] \end{aligned} \quad (D5)$$

First:

$$\begin{aligned} \text{Var}_\Theta[\delta_i^\lambda (-\sin(\theta_i) \zeta_i^\lambda + \cos(\theta_i) \zeta_j^\lambda)] &= \text{Var}_\Theta[2(\cos(\theta_i) \cdot \zeta_i^\lambda + \sin(\theta_i) \cdot \zeta_j^\lambda - \tilde{y}_i) \cdot (-\sin(\theta_i) \zeta_i^\lambda + \cos(\theta_i) \zeta_j^\lambda)] \\ &= 4 \int_{\Theta \in \Omega} \left(\frac{1}{2\pi}\right)^D (\delta_i^\lambda (-\sin(\theta_i) \zeta_i^\lambda + \cos(\theta_i) \zeta_j^\lambda) - \mathbb{E}_\Theta[\delta_i^\lambda (-\sin(\theta_i) \zeta_i^\lambda + \cos(\theta_i) \zeta_j^\lambda)])^2 d\Theta \end{aligned} \quad (D6)$$

With:

$$\begin{aligned} \mathbb{E}_\Theta[\delta_i^\lambda (-\sin(\theta_i) \zeta_i^\lambda + \cos(\theta_i) \zeta_j^\lambda)] &= \int_{\Theta \in \Omega} \left(\frac{1}{2\pi}\right)^D (2(\cos(\theta_i) \cdot \zeta_i^\lambda + \sin(\theta_i) \cdot \zeta_j^\lambda - \tilde{y}_i)) \cdot (-\sin(\theta_i) \zeta_i^\lambda + \cos(\theta_i) \zeta_j^\lambda) d\Theta \\ &= 2 \int_{\Theta \in \Omega} \left(\frac{1}{2\pi}\right)^D (\cos(\theta_i) \sin(\theta_i) ((\zeta_j^\lambda)^2 - (\zeta_i^\lambda)^2) d\Theta + 2 \int_{\Theta \in \Omega} \left(\frac{1}{2\pi}\right)^D (\cos^2(\theta_i) - \sin^2(\theta_i)) \zeta_j^\lambda \cdot \zeta_i^\lambda d\Theta \\ &\quad + 2 \int_{\Theta \in \Omega} \left(\frac{1}{2\pi}\right)^D (\sin(\theta_i) \cdot \zeta_i^\lambda - \cos(\theta_i) \cdot \zeta_j^\lambda) \tilde{y}_i d\Theta \end{aligned} \quad (D7)$$

According to our circuit decomposition into inner layers, the previous inner layer ζ^λ does not depend on the parameter θ_i but only on the previous parameters in the circuit. On the other hand, \tilde{y} does not depend on the parameter θ_i but only on the following parameters in the circuit. Thus, we can take out the integral according to θ_i :

$$\mathbb{E}_\Theta[\delta_i^\lambda (-\sin(\theta_i) \zeta_i^\lambda + \cos(\theta_i) \zeta_j^\lambda)] = 2 \int_{\Theta \in \Omega \setminus \theta_i} \left(\frac{1}{2\pi}\right)^D (\pi - \pi) \zeta_j^\lambda \cdot \zeta_i^\lambda d\Theta = 0 \quad (D8)$$

Therefore:

$$\begin{aligned} \text{Var}_\Theta[\delta_i^\lambda (-\sin(\theta_i) \zeta_i^\lambda + \cos(\theta_i) \zeta_j^\lambda)] &= 4 \int_{\Theta \in \Omega} \left(\frac{1}{2\pi}\right)^D (\delta_i^\lambda (-\sin(\theta_i) \zeta_i^\lambda + \cos(\theta_i) \zeta_j^\lambda))^2 d\Theta \\ &= 4 \int_{\Theta \in \Omega} \left(\frac{1}{2\pi}\right)^D [\cos^2(\theta_i) \sin^2(\theta_i) \cdot ((\zeta_j^\lambda)^2 - (\zeta_i^\lambda)^2)^2 + 2 \cos^3(\theta_i) \sin(\theta_i) \zeta_j^\lambda \zeta_i^\lambda ((\zeta_j^\lambda)^2 - (\zeta_i^\lambda)^2) \\ &\quad - 2 \cos(\theta_i) \sin^3(\theta_i) \zeta_j^\lambda \zeta_i^\lambda ((\zeta_j^\lambda)^2 - (\zeta_i^\lambda)^2) + 2 \cos(\theta_i) \sin^3(\theta_i) \zeta_i^\lambda ((\zeta_j^\lambda)^2 - (\zeta_i^\lambda)^2) \tilde{y}_i \\ &\quad - 2 \cos^2(\theta_i) \sin(\theta_i) \zeta_j^\lambda ((\zeta_j^\lambda)^2 - (\zeta_i^\lambda)^2) \tilde{y}_i + [\cos^4(\theta_i) - 2 \cos^2(\theta_i) \sin^2(\theta_i) + \sin^4(\theta_i)] (\zeta_i^\lambda)^2 (\zeta_j^\lambda)^2 \\ &\quad + 2 \cos^2(\theta_i) \sin(\theta_i) (\zeta_i^\lambda)^2 \zeta_j^\lambda \tilde{y}_i - 2 \sin^3(\theta_i) (\zeta_i^\lambda)^2 \zeta_j^\lambda \tilde{y}_i - 2 \cos^3(\theta_i) \zeta_i^\lambda (\zeta_j^\lambda)^2 \tilde{y}_i + 2 \cos(\theta_i) \sin^2(\theta_i) \zeta_i^\lambda (\zeta_j^\lambda)^2 \tilde{y}_i \\ &\quad + \sin^2(\theta_i) (\zeta_i^\lambda)^2 (\tilde{y}_i)^2 - 2 \cos(\theta_i) \sin(\theta_i) \zeta_i^\lambda \zeta_j^\lambda (\tilde{y}_i)^2 + \cos^2(\theta_i) (\zeta_j^\lambda)^2 (\tilde{y}_i)^2] d\Theta \\ &= 4 \int_{\Theta \in \Omega \setminus \theta_i} \left(\frac{1}{2\pi}\right)^D \left[\frac{\pi}{4} (\zeta_i^\lambda)^4 + \frac{\pi}{2} (\zeta_i^\lambda)^2 (\zeta_j^\lambda)^2 + \frac{\pi}{4} (\zeta_j^\lambda)^4 + \pi (\zeta_i^\lambda)^2 (\tilde{y}_i)^2 + \pi (\zeta_j^\lambda)^2 (\tilde{y}_i)^2 \right] d\Theta \end{aligned} \quad (D9)$$

Finally, we have:

$$\text{Var}_\Theta[\delta_i^\lambda (-\sin(\theta_i) \zeta_i^\lambda + \cos(\theta_i) \zeta_j^\lambda)] = \int_{\Theta \in \Omega} \left(\frac{1}{2\pi}\right)^D \left[\frac{1}{2} (\zeta_i^\lambda)^4 + (\zeta_i^\lambda)^2 (\zeta_j^\lambda)^2 + \frac{1}{2} (\zeta_j^\lambda)^4 + 2((\zeta_i^\lambda)^2 + (\zeta_j^\lambda)^2) (\tilde{y}_i)^2 \right] d\Theta \quad (D10)$$

With the same methods, it comes:

$$\text{Var}_{\Theta}[\delta_j^\lambda(-\cos(\theta_i)\zeta_i^\lambda - \sin(\theta_i)\zeta_j^\lambda)] = \int_{\Theta \in \Omega} \left(\frac{1}{2\pi}\right)^D \left[\frac{1}{2}(\zeta_i^\lambda)^4 + (\zeta_i^\lambda)^2(\zeta_j^\lambda)^2 + \frac{1}{2}(\zeta_j^\lambda)^4 + 2((\zeta_i^\lambda)^2 + (\zeta_j^\lambda)^2)(\tilde{y}_i)^2\right] d\Theta \quad (\text{D11})$$

We can decompose the covariance term:

$$\begin{aligned} \text{Cov}_{\Theta}[\delta_i^\lambda(-\sin(\theta_i)\zeta_i^\lambda + \cos(\theta_i)\zeta_j^\lambda); \delta_j^\lambda(-\cos(\theta_i)\zeta_i^\lambda - \sin(\theta_i)\zeta_j^\lambda)] \\ = \mathbb{E}_{\Theta}[\delta_i^\lambda(-\sin(\theta_i)\zeta_i^\lambda + \cos(\theta_i)\zeta_j^\lambda) \cdot \delta_j^\lambda(-\cos(\theta_i)\zeta_i^\lambda - \sin(\theta_i)\zeta_j^\lambda)] \\ - \mathbb{E}_{\Theta}[\delta_i^\lambda(-\sin(\theta_i)\zeta_i^\lambda + \cos(\theta_i)\zeta_j^\lambda)] \cdot \mathbb{E}_{\Theta}[\delta_j^\lambda(-\cos(\theta_i)\zeta_i^\lambda - \sin(\theta_i)\zeta_j^\lambda)] \end{aligned} \quad (\text{D12})$$

As shown with Eq.(D8):

$$\mathbb{E}_{\Theta}[\delta_i^\lambda(-\sin(\theta_i)\zeta_i^\lambda + \cos(\theta_i)\zeta_j^\lambda)] = \mathbb{E}_{\Theta}[\delta_j^\lambda(-\cos(\theta_i)\zeta_i^\lambda - \sin(\theta_i)\zeta_j^\lambda)] = 0 \quad (\text{D13})$$

Therefore, we have that the expectation value of the cost function gradient is null. In addition, we have:

$$\begin{aligned} \text{Cov}_{\Theta}[\delta_i^\lambda(-\sin(\theta_i)\zeta_i^\lambda + \cos(\theta_i)\zeta_j^\lambda); \delta_j^\lambda(-\cos(\theta_i)\zeta_i^\lambda - \sin(\theta_i)\zeta_j^\lambda)] \\ = \mathbb{E}_{\Theta}[\delta_i^\lambda(-\sin(\theta_i)\zeta_i^\lambda + \cos(\theta_i)\zeta_j^\lambda) \cdot \delta_j^\lambda(-\cos(\theta_i)\zeta_i^\lambda - \sin(\theta_i)\zeta_j^\lambda)] \\ = \int_{\Theta \in \Omega} \left(\frac{1}{2\pi}\right)^D [\delta_i^\lambda(-\sin(\theta_i)\zeta_i^\lambda + \cos(\theta_i)\zeta_j^\lambda) \cdot \delta_j^\lambda(-\cos(\theta_i)\zeta_i^\lambda - \sin(\theta_i)\zeta_j^\lambda)] d\Theta \\ = \int_{\Theta \in \Omega} \left(\frac{1}{2\pi}\right)^D [\cos^2(\theta_i) \sin^2(\theta_i) (-\zeta_i^\lambda)^4 + 2(\zeta_i^\lambda)^2(\zeta_j^\lambda)^2 - (\zeta_j^\lambda)^4 \\ + \cos(\theta_i) \sin(\theta_i) (\sin^2(\theta_i) - \cos^2(\theta_i)) ((\zeta_j^\lambda)^2 - (\zeta_i^\lambda)^2) \zeta_i^\lambda \zeta_j^\lambda + \cos^2(\theta_i) \sin(\theta_i) ((\zeta_j^\lambda)^2 - (\zeta_i^\lambda)^2) \zeta_i^\lambda \tilde{y}_j^\lambda \\ - \cos(\theta_i) \sin^2(\theta_i) ((\zeta_j^\lambda)^2 - (\zeta_i^\lambda)^2) \zeta_j^\lambda \tilde{y}_j^\lambda + \cos(\theta_i) \sin(\theta_i) (\cos^2(\theta_i) - \sin^2(\theta_i)) ((\zeta_j^\lambda)^2 - (\zeta_i^\lambda)^2) \zeta_i^\lambda \zeta_j^\lambda \\ - (\cos^4(\theta_i) - 2\cos^2(\theta_i) \sin^2(\theta_i) + \sin^4(\theta_i)) (\zeta_i^\lambda \zeta_j^\lambda)^2 + \cos(\theta_i) (\cos^2(\theta_i) - \sin^2(\theta_i)) (\zeta_i^\lambda)^2 \zeta_j^\lambda \tilde{y}_j^\lambda \\ = -\sin(\theta_i) (\cos^2(\theta_i) - \sin^2(\theta_i)) \zeta_i^\lambda (\zeta_j^\lambda)^2 \tilde{y}_j^\lambda + \cos(\theta_i) \sin^2(\theta_i) ((\zeta_j^\lambda)^2 - (\zeta_i^\lambda)^2) \zeta_i^\lambda \tilde{y}_i^\lambda \\ + \sin(\theta_i) (\sin^2(\theta_i) - \cos^2(\theta_i)) (\zeta_i^\lambda)^2 \zeta_j^\lambda \tilde{y}_i^\lambda + \cos(\theta_i) \sin(\theta_i) (\zeta_i^\lambda)^2 \tilde{y}_i^\lambda \tilde{y}_j^\lambda - \sin^2(\theta_i) \zeta_i^\lambda \zeta_j^\lambda \tilde{y}_i^\lambda \tilde{y}_j^\lambda \\ - \cos^2(\theta_i) \sin(\theta_i) ((\zeta_i^\lambda)^2 - (\zeta_j^\lambda)^2) \zeta_j^\lambda \tilde{y}_i^\lambda - \cos(\theta_i) (\sin^2(\theta_i) - \cos^2(\theta_i)) \zeta_i^\lambda (\zeta_j^\lambda)^2 \tilde{y}_i^\lambda \\ + \cos^2(\theta_i) \zeta_i^\lambda \zeta_j^\lambda \tilde{y}_i^\lambda \tilde{y}_j^\lambda + \cos(\theta_i) \sin(\theta_i) \zeta_j^\lambda \tilde{y}_i^\lambda \tilde{y}_j^\lambda] d\Theta \\ = -\frac{1}{2} \int_{\Theta \in \Omega} \left(\frac{1}{2\pi}\right)^D (\zeta_i^\lambda)^4 d\Theta - \frac{1}{2} \int_{\Theta \in \Omega} \left(\frac{1}{2\pi}\right)^D (\zeta_j^\lambda)^4 d\Theta - \int_{\Theta \in \Omega} \left(\frac{1}{2\pi}\right)^D (\zeta_i^\lambda)^2 (\zeta_j^\lambda)^2 d\Theta \end{aligned} \quad (\text{D14})$$

We can derive the variance of the cost gradient:

$$\begin{aligned} \text{Var}_{\Theta}[\partial_{\theta_i} \mathcal{C}(\Theta)] &= \text{Var}_{\Theta}[\delta_i^\lambda(-\sin(\theta_i)\zeta_i^\lambda + \cos(\theta_i)\zeta_j^\lambda)] + \text{Var}_{\Theta}[\delta_j^\lambda(-\cos(\theta_i)\zeta_i^\lambda - \sin(\theta_i)\zeta_j^\lambda)] \\ &\quad + 2 \cdot \text{Cov}_{\Theta}[\delta_i^\lambda(-\sin(\theta_i)\zeta_i^\lambda + \cos(\theta_i)\zeta_j^\lambda); \delta_j^\lambda(-\cos(\theta_i)\zeta_i^\lambda - \sin(\theta_i)\zeta_j^\lambda)] \\ &= \int_{\Theta \in \Omega} \left(\frac{1}{2\pi}\right)^D \left[\frac{1}{2}(\zeta_i^\lambda)^4 + (\zeta_i^\lambda)^2(\zeta_j^\lambda)^2 + \frac{1}{2}(\zeta_j^\lambda)^4 + 2((\zeta_i^\lambda)^2 + (\zeta_j^\lambda)^2)(\tilde{y}_i)^2\right] d\Theta \\ &\quad + \int_{\Theta \in \Omega} \left(\frac{1}{2\pi}\right)^D \left[\frac{1}{2}(\zeta_i^\lambda)^4 + (\zeta_i^\lambda)^2(\zeta_j^\lambda)^2 + \frac{1}{2}(\zeta_j^\lambda)^4 + 2((\zeta_i^\lambda)^2 + (\zeta_j^\lambda)^2)(\tilde{y}_i)^2\right] d\Theta \\ &\quad - \int_{\Theta \in \Omega} \left(\frac{1}{2\pi}\right)^D (\zeta_i^\lambda)^4 d\Theta - \int_{\Theta \in \Omega} \left(\frac{1}{2\pi}\right)^D (\zeta_j^\lambda)^4 d\Theta - 2 \int_{\Theta \in \Omega} \left(\frac{1}{2\pi}\right)^D (\zeta_i^\lambda)^2 (\zeta_j^\lambda)^2 d\Theta \end{aligned} \quad (\text{D15})$$

We find that:

$$\text{Var}_{\Theta}[\partial_{\theta_i} \mathcal{C}(\Theta)] = 2 \left(\int_{\Theta \in \Omega} \left(\frac{1}{2\pi}\right)^D (\zeta_i^\lambda)^2 + (\zeta_j^\lambda)^2 d\Theta \right) \cdot \left(\int_{\Theta \in \Omega} \left(\frac{1}{2\pi}\right)^D (\tilde{y}_i^\lambda)^2 + (\tilde{y}_j^\lambda)^2 d\Theta \right) \quad (\text{D16})$$

We claim that, if the initial state ζ_0 and the wanted output y are uniformly distributed on the basis B_1^n , we have that:

$$\forall \lambda, \forall r \in [n], \quad \int_{\Theta \in \Omega} \left(\frac{1}{2\pi}\right)^D (\zeta_r^\lambda)^2 d\Theta = \frac{1}{n} \quad (\text{D17})$$

We prove our claim using mathematical induction. First state case:

$$\forall r \in [n], \quad \int_{\Theta \in \Omega} \left(\frac{1}{2\pi}\right)^D (\zeta_r^0)^2 d\Theta = (\zeta_r^0)^2 \int_{\Theta \in \Omega} \left(\frac{1}{2\pi}\right)^D d\Theta = (\zeta_r^0)^2 = \frac{1}{n} \quad (\text{D18})$$

This result comes from the initial state independence of theta and its uniform distribution on the unary basis. We now suppose that the property given by Eq.(D17) is true for a given step λ . Then:

$$\forall r \in [n], \quad \int_{\Theta \in \Omega} \left(\frac{1}{2\pi}\right)^D (\zeta_r^{\lambda+1})^2 d\Theta = \begin{cases} \frac{1}{2} \int_{\Theta \in \Omega} \left(\frac{1}{2\pi}\right)^D (\zeta_{r,r'}^\lambda)^2 d\Theta + \frac{1}{2} \int_{\Theta \in \Omega} \left(\frac{1}{2\pi}\right)^D (\zeta_{r',r}^\lambda)^2 d\Theta \\ \int_{\Theta \in \Omega} \left(\frac{1}{2\pi}\right)^D (\zeta_r^\lambda)^2 d\Theta \end{cases} \quad (\text{D19})$$

The first case is when the state $|e_r\rangle$ was involved in a rotation by the application of the RBS between the inner layer λ and $\lambda + 1$. The second case correspond to a RBS that does not affect the state $|r\rangle$. In the two cases, we have:

$$\forall r \in [n], \quad \int_{\Theta \in \Omega} \left(\frac{1}{2\pi}\right)^D (\zeta_r^{\lambda+1})^2 d\Theta = \frac{1}{n} \quad (\text{D20})$$

Using the same method we can prove that, if the wanted output is uniformly distributed on the basis B_1^n , we have:

$$\forall \lambda, \forall r \in [n], \quad \int_{\Theta \in \Omega} \left(\frac{1}{2\pi}\right)^D (\tilde{y}_r^\lambda)^2 d\Theta = \frac{1}{n} \quad (\text{D21})$$

We can thus conclude that:

$$\text{Var}_{\Theta}[\partial_{\theta_i} \mathcal{C}(\Theta)] = 2 \left(\int_{\Theta \in \Omega} \left(\frac{1}{2\pi}\right)^D (\zeta_i^\lambda)^2 + (\zeta_j^\lambda)^2 d\Theta \right) \cdot \left(\int_{\Theta \in \Omega} \left(\frac{1}{2\pi}\right)^D (\tilde{y}_i^\lambda)^2 + (\tilde{y}_j^\lambda)^2 d\Theta \right) \approx \frac{8}{n^2} \quad (\text{D22})$$

We use the approximation sign because we are considering the expectation according to the input and output vectors.

2. Extension to any HW for RBS based VQC

We consider once again the case of the quadratic cost function. We call Δ^L the final error:

$$\Delta^L = 2(z^L - y) = 2[(w^{\lambda_{max}} \dots w^{\lambda+1}) \cdot w^\lambda \cdot \zeta^\lambda - y] \quad (\text{D23})$$

We still consider the case where for each inner layer, there is only one RBS gate considered. For each inner layer, the action of the gate results in a rotation of the amplitudes between a set of pair of states that we call \mathcal{R}_λ :

$$\zeta^{\lambda+1} = \overrightarrow{cst} + \sum_{(l,j) \in \mathcal{R}_\lambda} (\cos(\theta_i) \cdot \zeta_l^\lambda + \sin(\theta_i) \cdot \zeta_j^\lambda) |e_l\rangle + (-\sin(\theta_i) \cdot \zeta_l^\lambda + \cos(\theta_i) \cdot \zeta_j^\lambda) |e_j\rangle \quad (\text{D24})$$

with $\forall (l,j) \in \mathcal{R}_\lambda, \quad \overrightarrow{cst} \cdot |e_j\rangle = \overrightarrow{cst} \cdot |e_l\rangle = 0$

For example, the action of a RBS with parameter θ_i in B_2^n on the two first qubits of a 4-qubit quantum circuit results in the θ_i -planar rotation between the states $|1010\rangle$ and $|0110\rangle$, but also in the same θ_i -planar rotation between the states $|1001\rangle$ and $|0101\rangle$.

We can define the error according to the final error:

$$\begin{aligned} \delta^{\lambda+1} &= (w^{\lambda+1})^{-1} \dots (w^{\lambda_{max}})^{-1} \cdot \Delta^L = 2[w^\lambda \cdot \zeta^\lambda - (w^{\lambda+1})^{-1} \dots (w^{\lambda_{max}})^{-1} \cdot y] \\ &= 2[\overrightarrow{cst} + \sum_{(l,j) \in \mathcal{R}_\lambda} (\cos(\theta_i) \cdot \zeta_l^\lambda + \sin(\theta_i) \cdot \zeta_j^\lambda) |e_l\rangle + (-\sin(\theta_i) \cdot \zeta_l^\lambda + \cos(\theta_i) \cdot \zeta_j^\lambda) |e_j\rangle - \tilde{y}^\lambda] \end{aligned} \quad (\text{D25})$$

A unique RBS affects $\binom{n-2}{k-1}$ different pairs of states with a rotation, and all the affected states are different. As before, we have:

$$\forall (l,j) \in \mathcal{R}_\lambda, \quad \delta_i^{\lambda+1} = 2[\cos(\theta_i) \cdot \zeta_l^\lambda + \sin(\theta_i) \cdot \zeta_j^\lambda - \tilde{y}_l^\lambda] \quad (\text{D26})$$

and,

$$\forall (l,j) \in \mathcal{R}_\lambda, \quad \delta_j^{\lambda+1} = 2[-\sin(\theta_i) \cdot \zeta_l^\lambda + \cos(\theta_i) \cdot \zeta_j^\lambda - \tilde{y}_j^\lambda] \quad (\text{D27})$$

According to Theorem 3: $\forall \lambda, (w^\lambda)^{-1} = (w^\lambda)^t$.

We call: $\tilde{y} = (w^{\lambda+1})^t \dots (w^{\lambda_{max}})^t \cdot y$ and $\Omega = [0 : 2\pi]^D$ In the following, we will omit to note the set \mathcal{R}_λ .

$$\begin{aligned}
\text{Var}_\Theta[\partial_{\theta_i} \mathcal{C}] &= \text{Var}_\Theta\left[\sum_{(l,j)} \delta_l^\lambda (-\sin(\theta_i) \zeta_l^\lambda + \cos(\theta_i) \zeta_j^\lambda) + \delta_j^\lambda (-\cos(\theta_i) \zeta_l^\lambda - \sin(\theta_i) \zeta_j^\lambda)\right] \\
&= \sum_{(l,j)} \text{Var}_\Theta[\delta_l^\lambda (-\sin(\theta_i) \zeta_l^\lambda + \cos(\theta_i) \zeta_j^\lambda) + \delta_j^\lambda (-\cos(\theta_i) \zeta_l^\lambda - \sin(\theta_i) \zeta_j^\lambda)] \\
&\quad + 2 \sum_{(a,b) \neq (c,d)} \text{Cov}_\Theta[\delta_a^\lambda (-\sin(\theta_i) \zeta_a^\lambda + \cos(\theta_i) \zeta_b^\lambda) + \delta_b^\lambda (-\cos(\theta_i) \zeta_a^\lambda - \sin(\theta_i) \zeta_b^\lambda), \\
&\quad \delta_c^\lambda (-\sin(\theta_i) \zeta_c^\lambda + \cos(\theta_i) \zeta_d^\lambda) + \delta_d^\lambda (-\cos(\theta_i) \zeta_c^\lambda - \sin(\theta_i) \zeta_d^\lambda)]
\end{aligned} \tag{D28}$$

Using previous result from the previous Section D 1, we have:

$$\text{Var}_\Theta[\partial_{\theta_i} \mathcal{C}(\Theta)] = 2 \left(\int_{\Theta \in \Omega} \left(\frac{1}{2\pi} \right)^D (\zeta_l^\lambda)^2 + (\zeta_j^\lambda)^2 d\Theta \right) \cdot \left(\int_{\Theta \in \Omega} \left(\frac{1}{2\pi} \right)^D (\tilde{y}_l^\lambda)^2 + (\tilde{y}_j^\lambda)^2 d\Theta \right) \tag{D29}$$

Then,

$$\begin{aligned}
\text{Cov}_\Theta[\delta_a^\lambda (-\sin(\theta_i) \zeta_a^\lambda + \cos(\theta_i) \zeta_b^\lambda) + \delta_b^\lambda (-\cos(\theta_i) \zeta_a^\lambda - \sin(\theta_i) \zeta_b^\lambda), \\
\delta_c^\lambda (-\sin(\theta_i) \zeta_c^\lambda + \cos(\theta_i) \zeta_d^\lambda) + \delta_d^\lambda (-\cos(\theta_i) \zeta_c^\lambda - \sin(\theta_i) \zeta_d^\lambda)] \\
= \mathbb{E}_\Theta[(\delta_a^\lambda (-\sin(\theta_i) \zeta_a^\lambda + \cos(\theta_i) \zeta_b^\lambda) + \delta_b^\lambda (-\cos(\theta_i) \zeta_a^\lambda - \sin(\theta_i) \zeta_b^\lambda)) \cdot \\
(\delta_c^\lambda (-\sin(\theta_i) \zeta_c^\lambda + \cos(\theta_i) \zeta_d^\lambda) + \delta_d^\lambda (-\cos(\theta_i) \zeta_c^\lambda - \sin(\theta_i) \zeta_d^\lambda))] \\
- \mathbb{E}_\Theta[\delta_a^\lambda (-\sin(\theta_i) \zeta_a^\lambda + \cos(\theta_i) \zeta_b^\lambda) + \delta_b^\lambda (-\cos(\theta_i) \zeta_a^\lambda - \sin(\theta_i) \zeta_b^\lambda)] \cdot \\
\mathbb{E}_\Theta[\delta_c^\lambda (-\sin(\theta_i) \zeta_c^\lambda + \cos(\theta_i) \zeta_d^\lambda) + \delta_d^\lambda (-\cos(\theta_i) \zeta_c^\lambda - \sin(\theta_i) \zeta_d^\lambda)]
\end{aligned} \tag{D30}$$

Using previous result from the previous Section D 1 we have:

$$\begin{aligned}
\mathbb{E}_\Theta[\delta_a^\lambda (-\sin(\theta_i) \zeta_a^\lambda + \cos(\theta_i) \zeta_b^\lambda) + \delta_b^\lambda (-\cos(\theta_i) \zeta_a^\lambda - \sin(\theta_i) \zeta_b^\lambda)] \\
= \mathbb{E}_\Theta[\delta_c^\lambda (-\sin(\theta_i) \zeta_c^\lambda + \cos(\theta_i) \zeta_d^\lambda) + \delta_d^\lambda (-\cos(\theta_i) \zeta_c^\lambda - \sin(\theta_i) \zeta_d^\lambda)] \\
= 0
\end{aligned} \tag{D31}$$

We can now derive the value of the covariance term:

$$\begin{aligned}
\text{Cov}_\Theta[\delta_a^\lambda (-\sin(\theta_i) \zeta_a^\lambda + \cos(\theta_i) \zeta_b^\lambda) + \delta_b^\lambda (-\cos(\theta_i) \zeta_a^\lambda - \sin(\theta_i) \zeta_b^\lambda), \\
\delta_c^\lambda (-\sin(\theta_i) \zeta_c^\lambda + \cos(\theta_i) \zeta_d^\lambda) + \delta_d^\lambda (-\cos(\theta_i) \zeta_c^\lambda - \sin(\theta_i) \zeta_d^\lambda)] \\
= \mathbb{E}_\Theta[(\delta_a^\lambda (-\sin(\theta_i) \zeta_a^\lambda + \cos(\theta_i) \zeta_b^\lambda) + \delta_b^\lambda (-\cos(\theta_i) \zeta_a^\lambda - \sin(\theta_i) \zeta_b^\lambda)) \cdot \\
(\delta_c^\lambda (-\sin(\theta_i) \zeta_c^\lambda + \cos(\theta_i) \zeta_d^\lambda) + \delta_d^\lambda (-\cos(\theta_i) \zeta_c^\lambda - \sin(\theta_i) \zeta_d^\lambda))] \\
= \mathbb{E}_\Theta[\delta_a^\lambda (-\sin(\theta_i) \zeta_a^\lambda + \cos(\theta_i) \zeta_b^\lambda) \cdot \delta_c^\lambda (-\sin(\theta_i) \zeta_c^\lambda + \cos(\theta_i) \zeta_d^\lambda)] \\
+ \mathbb{E}_\Theta[\delta_a^\lambda (-\sin(\theta_i) \zeta_a^\lambda + \cos(\theta_i) \zeta_b^\lambda) \cdot \delta_d^\lambda (-\cos(\theta_i) \zeta_c^\lambda - \sin(\theta_i) \zeta_d^\lambda)] \\
+ \mathbb{E}_\Theta[\delta_b^\lambda (-\cos(\theta_i) \zeta_a^\lambda - \sin(\theta_i) \zeta_b^\lambda) \cdot \delta_c^\lambda (-\sin(\theta_i) \zeta_c^\lambda + \cos(\theta_i) \zeta_d^\lambda)] \\
+ \mathbb{E}_\Theta[\delta_b^\lambda (-\cos(\theta_i) \zeta_a^\lambda - \sin(\theta_i) \zeta_b^\lambda) \cdot \delta_d^\lambda (-\cos(\theta_i) \zeta_c^\lambda - \sin(\theta_i) \zeta_d^\lambda)]
\end{aligned} \tag{D32}$$

Using the integral expression of the expectation value:

$$\begin{aligned}
\mathbb{E}_\Theta[\delta_a^\lambda (-\sin(\theta_i) \zeta_a^\lambda + \cos(\theta_i) \zeta_b^\lambda) \cdot \delta_c^\lambda (-\sin(\theta_i) \zeta_c^\lambda + \cos(\theta_i) \zeta_d^\lambda)] \\
= \int_{\Theta \in \Omega} \left(\frac{1}{2\pi} \right)^D \left[\frac{1}{2} ((\zeta_b^\lambda)^2 (\zeta_d^\lambda)^2 - (\zeta_b^\lambda)^2 (\zeta_c^\lambda)^2 - (\zeta_a^\lambda)^2 (\zeta_d^\lambda)^2 + (\zeta_a^\lambda)^2 (\zeta_c^\lambda)^2) \right. \\
\left. + 2\zeta_a^\lambda \zeta_b^\lambda \zeta_c^\lambda \zeta_d^\lambda + 2\zeta_a^\lambda \zeta_c^\lambda \tilde{y}_a^\lambda \tilde{y}_c^\lambda + 2\zeta_b^\lambda \zeta_d^\lambda \tilde{y}_a^\lambda \tilde{y}_c^\lambda \right] d\Theta
\end{aligned} \tag{D33}$$

$$\begin{aligned}
\mathbb{E}_\Theta[\delta_a^\lambda (-\sin(\theta_i) \zeta_a^\lambda + \cos(\theta_i) \zeta_b^\lambda) \cdot \delta_d^\lambda (-\cos(\theta_i) \zeta_c^\lambda - \sin(\theta_i) \zeta_d^\lambda)] \\
= \int_{\Theta \in \Omega} \left(\frac{1}{2\pi} \right)^D \left[\frac{1}{2} ((\zeta_b^\lambda)^2 (\zeta_c^\lambda)^2 - (\zeta_a^\lambda)^2 (\zeta_c^\lambda)^2 - (\zeta_b^\lambda)^2 (\zeta_d^\lambda)^2 + (\zeta_a^\lambda)^2 (\zeta_d^\lambda)^2) \right. \\
\left. - 2\zeta_a^\lambda \zeta_b^\lambda \zeta_c^\lambda \zeta_d^\lambda + 2\zeta_a^\lambda \zeta_d^\lambda \tilde{y}_a^\lambda \tilde{y}_d^\lambda + 2\zeta_b^\lambda \zeta_c^\lambda \tilde{y}_a^\lambda \tilde{y}_d^\lambda \right] d\Theta
\end{aligned} \tag{D34}$$

$$\begin{aligned}
& \mathbb{E}_\Theta [\delta_b^\lambda (-\cos(\theta_i)\zeta_a^\lambda - \sin(\theta_i)\zeta_b^\lambda) \cdot \delta_c^\lambda (-\sin(\theta_i)\zeta_c^\lambda + \cos(\theta_i)\zeta_d^\lambda)] \\
&= \int_{\Theta \in \Omega} \left(\frac{1}{2\pi}\right)^D \left[\frac{1}{2} \left((\zeta_a^\lambda)^2 (\zeta_d^\lambda)^2 - (\zeta_b^\lambda)^2 (\zeta_d^\lambda)^2 - (\zeta_a^\lambda)^2 (\zeta_c^\lambda)^2 + (\zeta_b^\lambda)^2 (\zeta_c^\lambda)^2 \right) \right. \\
&\quad \left. - 2\zeta_a^\lambda \zeta_b^\lambda \zeta_c^\lambda \zeta_d^\lambda + 2\zeta_a^\lambda \zeta_d^\lambda \tilde{y}_b^\lambda \tilde{y}_c^\lambda + 2\zeta_b^\lambda \zeta_c^\lambda \tilde{y}_a^\lambda \tilde{y}_d^\lambda \right] d\Theta
\end{aligned} \tag{D35}$$

$$\begin{aligned}
& \mathbb{E}_\Theta [\delta_b^\lambda (-\cos(\theta_i)\zeta_a^\lambda - \sin(\theta_i)\zeta_b^\lambda) \cdot \delta_d^\lambda (-\cos(\theta_i)\zeta_c^\lambda - \sin(\theta_i)\zeta_d^\lambda)] \\
&= \int_{\Theta \in \Omega} \left(\frac{1}{2\pi}\right)^D \left[\frac{1}{2} \left((\zeta_a^\lambda)^2 (\zeta_c^\lambda)^2 - (\zeta_a^\lambda)^2 (\zeta_d^\lambda)^2 - (\zeta_b^\lambda)^2 (\zeta_c^\lambda)^2 + (\zeta_b^\lambda)^2 (\zeta_d^\lambda)^2 \right) \right. \\
&\quad \left. - 2\zeta_a^\lambda \zeta_b^\lambda \zeta_c^\lambda \zeta_d^\lambda + 2\zeta_a^\lambda \zeta_c^\lambda \tilde{y}_b^\lambda \tilde{y}_d^\lambda + 2\zeta_b^\lambda \zeta_d^\lambda \tilde{y}_a^\lambda \tilde{y}_c^\lambda \right] d\Theta
\end{aligned} \tag{D36}$$

By summing the terms:

$$\begin{aligned}
& \mathbb{Cov}_\Theta [\delta_a^\lambda (-\sin(\theta_i)\zeta_a^\lambda + \cos(\theta_i)\zeta_b^\lambda) + \delta_b^\lambda (-\cos(\theta_i)\zeta_a^\lambda - \sin(\theta_i)\zeta_b^\lambda), \\
&\quad \delta_c^\lambda (-\sin(\theta_i)\zeta_c^\lambda + \cos(\theta_i)\zeta_d^\lambda) + \delta_d^\lambda (-\cos(\theta_i)\zeta_c^\lambda - \sin(\theta_i)\zeta_d^\lambda)] \\
&= 2 \int_{\Theta \in \Omega} \left(\frac{1}{2\pi}\right)^D [(\zeta_a^\lambda \zeta_c^\lambda - \zeta_b^\lambda \zeta_d^\lambda)(\tilde{y}_a^\lambda \tilde{y}_c^\lambda + \tilde{y}_b^\lambda \tilde{y}_d^\lambda) + (\zeta_a^\lambda \zeta_d^\lambda - \zeta_b^\lambda \zeta_c^\lambda)(\tilde{y}_a^\lambda \tilde{y}_d^\lambda + \tilde{y}_b^\lambda \tilde{y}_c^\lambda)] d\Theta
\end{aligned} \tag{D37}$$

Finally,

$$\begin{aligned}
\text{Var}_\Theta [\partial_{\theta_i} \mathcal{C}] &= 2 \sum_{(l,j)} \left(\int_{\Theta \in \Omega} \left(\frac{1}{2\pi}\right)^D (\zeta_l^\lambda)^2 + (\zeta_j^\lambda)^2 d\Theta \right) \cdot \left(\int_{\Theta \in \Omega} \left(\frac{1}{2\pi}\right)^D (\tilde{y}_l^\lambda)^2 + (\tilde{y}_j^\lambda)^2 d\Theta \right) \\
&\quad + 4 \sum_{(a,b) \neq (c,d)} \int_{\Theta \in \Omega} \left(\frac{1}{2\pi}\right)^D [(\zeta_a^\lambda \zeta_c^\lambda + \zeta_b^\lambda \zeta_d^\lambda)(\tilde{y}_a^\lambda \tilde{y}_c^\lambda + \tilde{y}_b^\lambda \tilde{y}_d^\lambda) + (\zeta_a^\lambda \zeta_d^\lambda - \zeta_b^\lambda \zeta_c^\lambda)(\tilde{y}_a^\lambda \tilde{y}_d^\lambda - \tilde{y}_b^\lambda \tilde{y}_c^\lambda)] d\Theta
\end{aligned} \tag{D38}$$

We now claim that the covariance term is null. To show this, we are about to use an induction proof to prove that $\forall \lambda, \forall a, b \in [d_k], \int_{\Theta \in \Omega} \left(\frac{1}{2\pi}\right)^D \zeta_a^\lambda \zeta_b^\lambda d\Theta = 0$. First for the basis:

$$\forall a, b \in [d_k], \quad \int_{\Theta \in \Omega} \left(\frac{1}{2\pi}\right)^D \zeta_a^0 \zeta_b^0 d\Theta = \zeta_a^0 \zeta_b^0 \int_{\Theta \in \Omega} \left(\frac{1}{2\pi}\right)^D d\Theta = \zeta_a^0 \zeta_b^0 \tag{D39}$$

Considering the expectation value on the input vectors X , it comes:

$$\forall a, b \in [d_k], \quad \mathbb{E}_X [\zeta_a^0 \zeta_b^0] = 0 \tag{D40}$$

For the induction part, we just need to use the recursive formula on the evolution of the inner states. Let us consider the property verified on then layer λ :

$$\forall a, b \in [d_k], \quad \int_{\Theta \in \Omega} \left(\frac{1}{2\pi}\right)^D \zeta_a^{\lambda+1} \zeta_b^{\lambda+1} d\Theta = \begin{cases} \frac{1}{2} \int_{\Theta \in \Omega} \left(\frac{1}{2\pi}\right)^D \zeta_{a,a'}^\lambda \zeta_{b,b'}^\lambda d\Theta + \frac{1}{2} \int_{\Theta \in \Omega} \left(\frac{1}{2\pi}\right)^D \zeta_{a',a}^\lambda \zeta_{b',b}^\lambda d\Theta = 0 \\ \int_{\Theta \in \Omega} \left(\frac{1}{2\pi}\right)^D (\pm \cos(\theta_i) \zeta_{a,a'}^\lambda \pm \sin(\theta_i) \zeta_{a',a}^\lambda) \zeta_b^\lambda d\Theta = 0 \\ \int_{\Theta \in \Omega} \left(\frac{1}{2\pi}\right)^D \zeta_a^\lambda (\pm \cos(\theta_i) \zeta_{b,b'}^\lambda \pm \sin(\theta_i) \zeta_{b',b}^\lambda) d\Theta = 0 \\ \int_{\Theta \in \Omega} \left(\frac{1}{2\pi}\right)^D \zeta_a^\lambda \zeta_b^\lambda d\Theta = 0 \end{cases} \tag{D41}$$

The first case corresponds to the situation where a and b are affected by a rotation in the previous layer λ . The second and the third case refer to situation where only one state between a and b is affected by a rotation in the previous layer. By integrating over the corresponding parameter, those value are null. Finally, we consider the case where none of them are affected by a rotation in the previous layer. In all the cases if $a \neq b$, the result is null due to the induction hypothesis.

We prove by induction that:

$$\forall \lambda, \forall a, b \in [d_k], \quad a \neq b \implies \int_{\Theta \in \Omega} \left(\frac{1}{2\pi}\right)^D \zeta_a^\lambda \zeta_b^\lambda d\Theta = 0 \tag{D42}$$

Which implies that the covariance term is equal to 0:

$$\sum_{(a,b) \neq (c,d)} \int_{\Theta \in \Omega} \left(\frac{1}{2\pi}\right)^D [(\zeta_a^\lambda \zeta_c^\lambda + \zeta_b^\lambda \zeta_d^\lambda)(\tilde{y}_a^\lambda \tilde{y}_c^\lambda + \tilde{y}_b^\lambda \tilde{y}_d^\lambda) + (\zeta_a^\lambda \zeta_d^\lambda - \zeta_b^\lambda \zeta_c^\lambda)(\tilde{y}_a^\lambda \tilde{y}_d^\lambda - \tilde{y}_b^\lambda \tilde{y}_c^\lambda)] d\Theta = 0 \quad (\text{D43})$$

Using the expectation of this value over the input and output vectors, we can show in a similar way as in the previous Section D 1 that:

$$\forall r \in [d_k], \quad \int_{\Theta \in \Omega} \left(\frac{1}{2\pi}\right)^D (\zeta_r^{\lambda+1})^2 d\Theta \approx \frac{1}{d_k} \quad (\text{D44})$$

and,

$$\forall \lambda, \forall r \in [d_k], \quad \int_{\Theta \in \Omega} \left(\frac{1}{2\pi}\right)^D (\tilde{y}_r^\lambda)^2 d\Theta \approx \frac{1}{d_k} \quad (\text{D45})$$

Using the expectation value on the input and wanted output distribution:

$$\text{Var}_\Theta[\partial_{\theta_i} \mathcal{C}] = 2 \sum_{(l,j)} \left(\int_{\Theta \in \Omega} \left(\frac{1}{2\pi}\right)^D (\zeta_l^\lambda)^2 + (\zeta_j^\lambda)^2 d\Theta \right) \cdot \left(\int_{\Theta \in \Omega} \left(\frac{1}{2\pi}\right)^D (\tilde{y}_l^\lambda)^2 + (\tilde{y}_j^\lambda)^2 d\Theta \right) = \sum_{(l,j)} \frac{8}{d_k^2} \quad (\text{D46})$$

The sum is over all the rotation induces by the RBS of variational parameter θ_i . The number of rotation between different couple of states is:

$$\binom{n-2}{k-1} = \frac{(n-2)!}{(k-1)!(n-1-k)!} = \frac{k(n-k)}{n(n-1)} \binom{n}{k} = \frac{k(n-k)}{n(n-1)} d_k \quad (\text{D47})$$

We conclude:

$$\text{Var}_\Theta[\partial_{\theta_i} \mathcal{C}] \approx \frac{k(n-k)}{n(n-1)} \frac{8}{d_k} \quad (\text{D48})$$

We prove Theorem 1 in the specific case of RBS gate. In the following section we show how to generalize this result for FBS gates.

3. Generalization for FBS gates

In this section, we explain how to adapt the previous proof given in Section D 2 to extend our result to FBS based quantum circuits.

We consider once again the case of the quadratic cost function. The decomposition of the FBS based quantum circuit for the backpropagation method is very similar to the case of RBS based quantum circuit:

We call Δ^L the final error:

$$\Delta^L = 2(z^L - y) = 2[(w^{\lambda_{max}} \dots w^{\lambda+1}) \cdot w^\lambda \cdot \zeta^\lambda - y] \quad (\text{D49})$$

We consider the case where for each inner layer, there is only one FBS gate considered. For each inner layer, the action of the gate results in a rotation of the amplitudes between a set of pair of states that we call \mathcal{R}_λ :

$$\zeta^{\lambda+1} = \overrightarrow{cst} + \sum_{(l,j) \in \mathcal{R}_\lambda} (\cos(\theta_i) \cdot \zeta_l^\lambda + (-1)^{f(l,j,\zeta_j^\lambda)} \sin(\theta_i) \cdot \zeta_j^\lambda) |e_l\rangle + ((-1)^{f(l,j,\zeta_l^\lambda)+1} \sin(\theta_i) \cdot \zeta_l^\lambda + \cos(\theta_i) \cdot \zeta_j^\lambda) |e_j\rangle \quad (\text{D50})$$

with $\forall (l,j) \in \mathcal{R}_\lambda, \quad \overrightarrow{cst}^t \cdot |e_j\rangle = \overrightarrow{cst}^t \cdot |e_l\rangle = 0$

We can define the error according to the final error:

$$\begin{aligned} \delta^{\lambda+1} &= (w^{\lambda+1})^{-1} \dots (w^{\lambda_{max}})^{-1} \cdot \Delta^L = 2[w^\lambda \cdot \zeta^\lambda - (w^{\lambda+1})^{-1} \dots (w^{\lambda_{max}})^{-1} \cdot y] \\ &= 2[\overrightarrow{cst} + \sum_{(l,j) \in \mathcal{R}_\lambda} (\cos(\theta_i) \cdot \zeta_l^\lambda + (-1)^{f(l,j,\zeta_j^\lambda)} \sin(\theta_i) \cdot \zeta_j^\lambda) |e_l\rangle \\ &\quad + ((-1)^{f(l,j,\zeta_l^\lambda)+1} \sin(\theta_i) \cdot \zeta_l^\lambda + \cos(\theta_i) \cdot \zeta_j^\lambda) |e_j\rangle - \tilde{y}^\lambda] \end{aligned} \quad (\text{D51})$$

A unique RBS affects $\binom{n-2}{k-1}$ different pairs of states with a rotation, and all the affected states are different. A unique FBS applied on the same qubits affects the same pairs of states. Therefore:

$$\forall (l, j) \in \mathcal{R}_\lambda, \quad \delta_l^{\lambda+1} = 2[\cos(\theta_i) \cdot \zeta_l^\lambda + (-1)^{f(l,j,\zeta_j^\lambda)} \sin(\theta_i) \cdot \zeta_j^\lambda - \tilde{y}_l^\lambda] \quad (\text{D52})$$

and,

$$\forall (l, j) \in \mathcal{R}_\lambda, \quad \delta_j^{\lambda+1} = 2[(-1)^{f(l,j,\zeta_l^\lambda)+1} \sin(\theta_i) \cdot \zeta_l^\lambda + \cos(\theta_i) \cdot \zeta_j^\lambda - \tilde{y}_j^\lambda] \quad (\text{D53})$$

According to Theorem 3: $\forall \lambda, \quad (w^\lambda)^{-1} = (w^\lambda)^t$.

We call: $\tilde{y} = (w^{\lambda+1})^t \dots (w^{\lambda_{max}})^t \cdot y$ and $\Omega = [0 : 2\pi]^D$. In the following, we will omit to note the set \mathcal{R}_λ .

$$\begin{aligned} \text{Var}_\Theta[\partial_{\theta_i} \mathcal{C}] &= \text{Var}_\Theta \left[\sum_{(l,j)} \delta_l^\lambda (-\sin(\theta_i) \zeta_l^\lambda + (-1)^{f(l,j,\zeta_j^\lambda)} \cos(\theta_i) \zeta_j^\lambda) + \delta_j^\lambda ((-1)^{f(l,j,\zeta_l^\lambda)} \cos(\theta_i) \zeta_l^\lambda - \sin(\theta_i) \zeta_j^\lambda) \right] \\ &= \sum_{(l,j)} \text{Var}_\Theta [\delta_l^\lambda (-\sin(\theta_i) \zeta_l^\lambda + (-1)^{f(l,j,\zeta_j^\lambda)} \cos(\theta_i) \zeta_j^\lambda) + \delta_j^\lambda ((-1)^{f(l,j,\zeta_l^\lambda)} \cos(\theta_i) \zeta_l^\lambda - \sin(\theta_i) \zeta_j^\lambda)] \\ &\quad + 2 \sum_{(a,b) \neq (c,d)} \text{Cov}_\Theta [\delta_a^\lambda (-\sin(\theta_i) \zeta_a^\lambda + (-1)^{f(a,b,\zeta_b^\lambda)} \cos(\theta_i) \zeta_b^\lambda) + \delta_b^\lambda ((-1)^{f(a,b,\zeta_a^\lambda)} \cos(\theta_i) \zeta_a^\lambda - \sin(\theta_i) \zeta_b^\lambda), \\ &\quad \delta_c^\lambda (-\sin(\theta_i) \zeta_c^\lambda + (-1)^{f(c,d,\zeta_d^\lambda)} \cos(\theta_i) \zeta_d^\lambda) + \delta_d^\lambda ((-1)^{f(c,d,\zeta_c^\lambda)} \cos(\theta_i) \zeta_c^\lambda - \sin(\theta_i) \zeta_d^\lambda)] \end{aligned} \quad (\text{D54})$$

The only change in comparison with the RBS case is with the sign of the sinus in the previous equations. However, in the proof of Theorem 1 given in the previous appendix, we derive each term of Eq.(D54) by integrating over the parameter θ_i . The sign of the sine does not change the integration and as a result we find again that:

$$\begin{aligned} \text{Var}_\Theta[\partial_{\theta_i} \mathcal{C}] &= 2 \sum_{(l,j)} \left(\int_{\Theta \in \Omega} \left(\frac{1}{2\pi} \right)^D (\zeta_l^\lambda)^2 + (\zeta_j^\lambda)^2 d\Theta \right) \cdot \left(\int_{\Theta \in \Omega} \left(\frac{1}{2\pi} \right)^D (\tilde{y}_l^\lambda)^2 + (\tilde{y}_j^\lambda)^2 d\Theta \right) \\ &\quad + 4 \sum_{(a,b) \neq (c,d)} \int_{\Theta \in \Omega} \left(\frac{1}{2\pi} \right)^D [(\zeta_a^\lambda \zeta_c^\lambda + \zeta_b^\lambda \zeta_d^\lambda) (\tilde{y}_a^\lambda \tilde{y}_c^\lambda + \tilde{y}_b^\lambda \tilde{y}_d^\lambda) + (\zeta_a^\lambda \zeta_d^\lambda - \zeta_b^\lambda \zeta_c^\lambda) (\tilde{y}_a^\lambda \tilde{y}_d^\lambda - \tilde{y}_b^\lambda \tilde{y}_c^\lambda)] d\Theta \end{aligned} \quad (\text{D55})$$

With the FBS, we consider the same induction relation between the inner layers than in the case of RBS based gates:

$$\forall r \in [d_k], \quad \int_{\Theta \in \Omega} \left(\frac{1}{2\pi} \right)^D (\zeta_r^{\lambda+1})^2 d\Theta = \begin{cases} \frac{1}{2} \int_{\Theta \in \Omega} \left(\frac{1}{2\pi} \right)^D (\zeta_{r,r'}^\lambda)^2 d\Theta + \frac{1}{2} \int_{\Theta \in \Omega} \left(\frac{1}{2\pi} \right)^D (\zeta_{r',r}^\lambda)^2 d\Theta \\ \int_{\Theta \in \Omega} \left(\frac{1}{2\pi} \right)^D (\zeta_r^\lambda)^2 d\Theta \end{cases} \quad (\text{D56})$$

We can thus consider in a similar way that the covariance term is null. Using the expectation of this value over the input and output vectors, we can show in a similar way as in the previous Section D2, that:

$$\forall r \in [d_k], \quad \int_{\Theta \in \Omega} \left(\frac{1}{2\pi} \right)^D (\zeta_r^{\lambda+1})^2 d\Theta \approx \frac{1}{d_k} \quad (\text{D57})$$

and,

$$\forall \lambda, \forall r \in [d_k], \quad \int_{\Theta \in \Omega} \left(\frac{1}{2\pi} \right)^D (\tilde{y}_r^\lambda)^2 d\Theta \approx \frac{1}{d_k} \quad (\text{D58})$$

Using the expectation value on the input and wanted output distribution:

$$\text{Var}_\Theta[\partial_{\theta_i} \mathcal{C}] = 2 \sum_{(l,j)} \left(\int_{\Theta \in \Omega} \left(\frac{1}{2\pi} \right)^D (\zeta_l^\lambda)^2 + (\zeta_j^\lambda)^2 d\Theta \right) \cdot \left(\int_{\Theta \in \Omega} \left(\frac{1}{2\pi} \right)^D (\tilde{y}_l^\lambda)^2 + (\tilde{y}_j^\lambda)^2 d\Theta \right) = \sum_{(l,j)} \frac{8}{d_k^2} \quad (\text{D59})$$

The sum is over all the rotation induces by the RBS of variational parameter θ_i . The number of rotation between different couple of states is unchanged:

$$\binom{n-2}{k-1} = \frac{(n-2)!}{(k-1)!(n-1-k)!} = \frac{k(n-k)}{n(n-1)} \binom{n}{k} = \frac{k(n-k)}{n(n-1)} d_k \quad (\text{D60})$$

We conclude:

$$\mathbb{V}ar_{\Theta}[\partial_{\theta_i} \mathcal{C}] \approx \frac{k(n-k)}{n(n-1)} \frac{8}{d_k} \quad (\text{D61})$$

Therefore, we prove the **Theorem 1**.

Appendix E: Proof of Theorem 2

We recall the **Theorem 2**:

Theorem 2 (Evolution of the variance for RBS and FBS based quantum data loader). *Let us consider a n -qubit HW preserving VQC made of RBS or FBS gate. We consider here the subspace of HW k , i.e. corresponding to the basis B_k^n . If the initial state is a single state $|e_s\rangle \in B_k^n$ and the wanted output is Haar distributed on the basis B_k^n , we have that:*

$$\forall i \geq \lambda_0, \quad \mathbb{E}_{\Theta}[\partial_{\theta_i} \mathcal{C}(\Theta)] = 0, \quad \mathbb{V}ar_{\Theta}[\partial_{\theta_i} \mathcal{C}(\Theta)] \approx \frac{k(n-k)}{n(n-1)} \frac{8}{d_k} \quad (\text{22})$$

with λ_0 is such that from the gate with variational parameter θ_{λ_0} every state in B_k^n can be reached. We recall that $d_k = \binom{n}{k}$.

As in the proof of **Theorem 1** presented previously, we can state for RBS or FBS that:

$$\begin{aligned} \mathbb{V}ar_{\Theta}[\partial_{\theta_i} \mathcal{C}] &= 2 \sum_{(l,j)} \left(\int_{\Theta \in \Omega} \left(\frac{1}{2\pi} \right)^D (\zeta_l^\lambda)^2 + (\zeta_j^\lambda)^2 d\Theta \right) \cdot \left(\int_{\Theta \in \Omega} \left(\frac{1}{2\pi} \right)^D (\tilde{y}_l^\lambda)^2 + (\tilde{y}_j^\lambda)^2 d\Theta \right) \\ &+ 4 \sum_{(a,b) \neq (c,d)} \int_{\Theta \in \Omega} \left(\frac{1}{2\pi} \right)^D [(\zeta_a^\lambda \zeta_c^\lambda + \zeta_b^\lambda \zeta_d^\lambda)(\tilde{y}_a^\lambda \tilde{y}_c^\lambda + \tilde{y}_b^\lambda \tilde{y}_d^\lambda) + (\zeta_a^\lambda \zeta_d^\lambda - \zeta_b^\lambda \zeta_c^\lambda)(\tilde{y}_a^\lambda \tilde{y}_d^\lambda - \tilde{y}_b^\lambda \tilde{y}_c^\lambda)] d\Theta \end{aligned} \quad (\text{E1})$$

Using the exact same type of induction proof as in **D 2**, we can prove that:

$$\forall \lambda, \forall a, b \in [d_k], \quad \int_{\Theta \in \Omega} \left(\frac{1}{2\pi} \right)^D \tilde{y}_a^\lambda \tilde{y}_b^\lambda d\Theta = 0 \quad (\text{E2})$$

Which implies that the covariance term is equal to 0 for any inner layer λ :

$$\sum_{(a,b) \neq (c,d)} \int_{\Theta \in \Omega} \left(\frac{1}{2\pi} \right)^D [(\zeta_a^\lambda \zeta_c^\lambda + \zeta_b^\lambda \zeta_d^\lambda)(\tilde{y}_a^\lambda \tilde{y}_c^\lambda + \tilde{y}_b^\lambda \tilde{y}_d^\lambda) + (\zeta_a^\lambda \zeta_d^\lambda - \zeta_b^\lambda \zeta_c^\lambda)(\tilde{y}_a^\lambda \tilde{y}_d^\lambda - \tilde{y}_b^\lambda \tilde{y}_c^\lambda)] d\Theta = 0 \quad (\text{E3})$$

We then just have:

$$\mathbb{V}ar_{\Theta}[\partial_{\theta_i} \mathcal{C}] = 2 \sum_{(l,j)} \left(\int_{\Theta \in \Omega} \left(\frac{1}{2\pi} \right)^D (\zeta_l^\lambda)^2 + (\zeta_j^\lambda)^2 d\Theta \right) \cdot \left(\int_{\Theta \in \Omega} \left(\frac{1}{2\pi} \right)^D (\tilde{y}_l^\lambda)^2 + (\tilde{y}_j^\lambda)^2 d\Theta \right) \quad (\text{E4})$$

By hypothesis on the wanted output distribution, we replace the integral of the \tilde{y} terms by its expectation value over the wanted output vectors:

$$\forall \lambda, \forall r \in [d_k], \quad \int_{\Theta \in \Omega} \left(\frac{1}{2\pi} \right)^D (\tilde{y}_r^\lambda)^2 d\Theta \approx \frac{1}{d_k} \quad (\text{E5})$$

We now consider a new distribution for our input vector:

$$\forall r \in [d_k], \quad \zeta_r^0 = \delta_{r,s} \quad \text{with } |e_s\rangle \text{ the initial state of our quantum circuit and } \delta_{r,s} \text{ the Kronecker function.} \quad (\text{E6})$$

We notice that we can express the integral for each state as a probability:

$$\forall \lambda, \quad \sum_{i \in [d_k]} \int_{\Omega} \left(\frac{1}{2\pi}\right)^D (\zeta_i^\lambda)^2 d\Theta = 1 \quad \text{and} \quad \forall i \in [d_k], \quad \int_{\Omega} \left(\frac{1}{2\pi}\right)^D (\zeta_i^\lambda)^2 d\Theta \in [0, 1] \quad (\text{E7})$$

If one picks randomly a couple of state in the basis B_k^n , we have **in average** (according to the state we choose):

$$\int_{\Theta \in \Omega} \left(\frac{1}{2\pi}\right)^D (\zeta_i^\lambda)^2 + (\zeta_j^\lambda)^2 d\Theta = \frac{2}{d_k} \quad (\text{E8})$$

However, we would like to now more about the exact value of

$$\int_{\Omega} \left(\frac{1}{2\pi}\right)^D (\zeta_i^\lambda)^2 d\Theta$$

For any $i \in [d_k]$. Let us consider a given state $|e_s\rangle$ and a given inner layer λ . If the state $|e_s\rangle$ is affected by a rotation due to the inner layer with another state $|e_r\rangle$, we have:

$$\int_{\Omega} \left(\frac{1}{2\pi}\right)^D (\zeta_s^{\lambda+1})^2 d\Theta = \frac{1}{2} \int_{\Omega} \left(\frac{1}{2\pi}\right)^D (\zeta_s^\lambda)^2 d\Theta + \frac{1}{2} \int_{\Omega} \left(\frac{1}{2\pi}\right)^D (\zeta_r^\lambda)^2 d\Theta \quad (\text{E9})$$

and:

$$\int_{\Omega} \left(\frac{1}{2\pi}\right)^D (\zeta_r^{\lambda+1})^2 d\Theta = \frac{1}{2} \int_{\Omega} \left(\frac{1}{2\pi}\right)^D (\zeta_s^\lambda)^2 d\Theta + \frac{1}{2} \int_{\Omega} \left(\frac{1}{2\pi}\right)^D (\zeta_r^\lambda)^2 d\Theta \quad (\text{E10})$$

Therefore, each RBS or FBS is keen to normalize the distribution of probabilities describe on Eq.(E7). Therefore if the circuit has enough gates that affected all the states in B_k^n , we can consider that:

$$\int_{\Omega} \left(\frac{1}{2\pi}\right)^D (\zeta_i^\lambda)^2 d\Theta \approx \frac{1}{d_k} \quad (\text{E11})$$

We call λ_0 the minimal number of gates (or inner states in the circuit decomposition) such as every state in B_k^n can be reached. This means that:

$$\forall \lambda \geq \lambda_0, \quad \forall r \in [d_k], \quad \exists \Theta \in [0, 2\pi]^D \setminus \zeta_r^\lambda \neq 0 \quad (\text{E12})$$

This implies that:

$$\forall \lambda \geq \lambda_0, \quad \forall r \in [d_k], \quad \int_{\Omega} \left(\frac{1}{2\pi}\right)^D (\zeta_i^\lambda)^2 d\Theta \neq 0 \quad (\text{E13})$$

Thus:

$$\forall i \geq \lambda_0, \quad \text{Var}_{\Theta}[\partial_{\theta_i} \mathcal{C}] \approx 2 \sum_{(l,j)} \frac{2}{d_k} \cdot \frac{2}{d_k} \quad (\text{E14})$$

Or the number of couple of states in the sum is $\binom{n-2}{k-1}$ and we have as shown previously that:

$$\binom{n-2}{k-1} = \frac{(n-2)!}{(k-1)!(n-1-k)!} = \frac{k(n-k)}{n(n-1)} \binom{n}{k} = \frac{k(n-k)}{n(n-1)} d_k \quad (\text{E15})$$

We can thus conclude using the hypothesis from Eq.(E11) that:

$$\forall i \geq \lambda_0, \quad \mathbb{E}_{\Theta}[\partial_{\theta_i} \mathcal{C}(\Theta)] = 0, \quad \text{Var}_{\Theta}[\partial_{\theta_i} \mathcal{C}(\Theta)] \approx \frac{k(n-k)}{n(n-1)} \frac{8}{d_k} \quad (\text{E16})$$